

**EFFECT OF DIFFERENT LASER POWER DENSITIES ON
EFFICIENCY OF PHOTOBIMODULATION OF MOUSE
FIBROBLASTS IN VITRO**

by

İpek DÜZGÖREN

B.Sc., Physics, Middle East Technical University, 2015

Submitted to the Institute of Biomedical Engineering
in partial fulfillment of the requirements
for the degree of
Master of Science
in
Biomedical Engineering

Boğaziçi University

2019

**EFFECT OF DIFFERENT LASER POWER DENSITIES ON
EFFICIENCY OF PHOTOBIOMODULATION OF MOUSE
FIBROBLASTS IN VITRO**

APPROVED BY:

Prof. Dr. Murat Gülsoy
(Thesis Advisor)

Assoc. Prof. Dr. Bora Garipcan

Assist. Prof. Dr. Hakan Solmaz

DATE OF APPROVAL: March 12 2019

ACKNOWLEDGMENTS

Foremost, I would like to thank my thesis advisor Prof. Dr. Murat Gülsoy for his useful feedbacks and remarks. Through the learning process of this thesis, he guided me in the right direction whenever he thought I need it. Also, I appreciate the feedback offered by the members of thesis committee.

I would also like to acknowledge Assoc. Prof. Dr. Bora Garipcan for his contributions to my study. When I looked for an alternative solution to advance my research, he showed me different perspectives. Besides, I would like to express my wholehearted thanks his group members for sharing their lab opportunities.

I owe my deepest gratitude to alumnus and current members of the Biophotonics Laboratory. I am particularly grateful to Dr. Mustafa Kemal Ruhi for his guidance and persistent help. I would also like to offer my special thanks to Özgür Kaya. He has taught me how become a good scientist.

I want to thank my true friends. All the time, they encourage me to realize my dreams. I would also like to thank my family members. Their endless love and support are always with me in the journey of life.

ACADEMIC ETHICS AND INTEGRITY STATEMENT

I, İpek Düzgören, hereby certify that I am aware of the Academic Ethics and Integrity Policy issued by the Council of Higher Education (YÖK) and I fully acknowledge all the consequences due to its violation by plagiarism or any other way.

Name :

Signature:

Date:

ABSTRACT

EFFECT OF DIFFERENT LASER POWER DENSITIES ON EFFICIENCY OF PHOTOBIMODULATION OF MOUSE FIBROBLASTS IN VITRO

The purpose of the present study was to investigate the efficiency of photobiomodulation (PBM) with respect to different energy and power densities, as well as different incubation times on fibroblast cells. Photobiomodulation (PBM) was performed with visible (VIS) laser light at a wavelength of 635 nm. Murine fibroblasts (L929 cell line) were irradiated at 50 mW/cm², 125 mW/cm², 200 mW/cm² of power densities, separately. Laser irradiation time was varied with respect to the selected power density to keep constant the energy density for the laser groups (i.e. 1 J/cm², 3 J/cm², and 5 J/cm²). Cell viabilities were determined by MTT (3-(4,5-Dimethyliazol-2-yl)-2,5 diphenyltetrazolium bromide) assay test. Results showed that photobiomodulation effect was determined by energy density, power density, and incubation time. It can be proliferative or none and even under some circumstances inhibitory. For future studies, same paradigm should be tested with in vivo models.

Keywords: Photobiomodulation (PBM), Power density, Photochemical reaction, Low level laser application, Proliferation, Optimal dose, Incubation time.

ÖZET

FARKLI LASER GÜÇ YOĞUNLUKLARININ İN VİTRO FARE FİBROBLASTLARININ FOTOBİYOMODÜLASYONU VERİMLİLİĞİNE ETKİSİ

Bu çalışmanın amacı, fotobiyomodülasyonun (PBM) farklı enerji ve güç yoğunluklarına ilaveten farklı inkübasyon süreleri açısından fibroblast hücrelerinde etkinliğini araştırmaktır. Fotobiyomodülasyon (PBM), 635 nm dalga boyunda görünür (VIS) laser ışığıyla gerçekleştirilmiştir. Fare fibroblastları (L929 hücre hattı), ayrı ayrı 50 mW/cm², 125 mW/cm², 200 mW/cm² güç yoğunluklarında ışınlanmıştır. Laser ışınım süresi, laser grupları için enerji yoğunluğunu ayrı ayrı 1 J/cm², 3 J/cm² ve 5 J/cm²'de sabit tutmak için seçilen güç yoğunluğuna göre değişmiştir. Hücre canlılığı, MTT (3-(4,5-Dimetiazol-2-il) -2,5 difeniltetrazolyum bromür) tahlil testi ile tespit edilmiştir. Sonuçlar, fotobiyomodülasyon etkisinin enerji yoğunluğu, güç yoğunluğu ve laser ışınımı sonrası inkübasyon süresi ile belirlendiğini göstermiştir. Sonuçların hücre canlılığına etkisi proliferatif olabilir veya hiçbir etki sağlamayabilir ve hatta bazı durumlarda inhibe edici olabilir. Gelecekteki çalışmalar için, aynı paradigma in vivo modellerle test edilmelidir.

Anahtar Sözcükler: Fotobiyomodülasyon, güç yoğunluğu, fotokimyasal reaksiyon, düşük dozlu laser uygulaması, proliferasyon, en uygun parametre, inkübasyon süresi.

TABLE OF CONTENTS

ACKNOWLEDGMENTS	iii
ACADEMIC ETHICS AND INTEGRITY STATEMENT	iv
ABSTRACT	v
ÖZET	vi
LIST OF FIGURES	ix
LIST OF TABLES	xi
LIST OF SYMBOLS	xii
LIST OF ABBREVIATIONS	xiii
1. INTRODUCTION	1
1.1 Motivation	1
1.2 Objectives	2
1.3 Outline	3
2. BACKGROUND	4
2.1 Fibroblast Cells	4
2.2 Cell Proliferation	5
2.3 Laser-Tissue Interactions	7
2.4 Photochemical Effect of Interaction between Tissue and Light	12
2.5 Photobiomodulation (PBM)	13
3. MATERIALS AND METHODS	25
3.1 Cell Culture	25
3.2 Laser Irradiation	27
3.3 Cell viability (MTT Assay)	30
3.4 Statistical Analysis	31
4. RESULTS AND DISCUSSIONS	32
4.1 The effect of PBM on L929 cell proliferation with 24 h incubation after laser irradiation	32
4.1.1 Irradiation at 50 mW/cm ²	32
4.1.2 Irradiation at 125 mW/cm ²	33
4.1.3 Irradiation at 200 mW/cm ²	34

4.2	The effect of PBM on L929 cell proliferation with 48 h incubation after laser irradiation	35
4.2.1	Irradiation at 50 mW/cm ²	35
4.2.2	Irradiation at 125 mW/cm ²	36
4.2.3	Irradiation at 200 mW/cm ²	37
4.3	The effect of PBM on L929 cell proliferation with 72 h incubation after laser irradiation	38
4.3.1	Irradiation at 50 mW/cm ²	38
4.3.2	Irradiation at 125 mW/cm ²	39
4.3.3	Irradiation at 200 mW/cm ²	40
4.4	Results Overview	41
4.5	Discussion	42
5.	CONCLUSION	47
	REFERENCES	49

LIST OF FIGURES

Figure 2.1	Illustration of dermatological layers and components of the skin [6].	4
Figure 2.2	Representation of photospectral range of main tissue absorbers of human skin and other tissue types [18].	8
Figure 2.3	The scheme which is Jablonski diagram of molecular energy levels of excitation, ionization, and relaxation shows principle of the light interaction with M molecule. The transition rates are indicated by straight lines which are radiative transition; waving and multi arrow lines are non-radiative [19].	9
Figure 2.4	Graphical representation of how light penetration is changed by wavelength [22].	10
Figure 2.5	Representation of effect of beam width on light penetration [22].	11
Figure 2.6	The scheme of interaction between laser light and cyt c molecule.	14
Figure 2.7	Assumed primary reactions in COX molecule after excitation of an atom from the ground state to the upper energy states. S1 is only figurative state, not obligatory. These are the hypothesis of Karu's studies: Redox properties alteration hypothesis (1998), NO hypothesis (2005), Superoxide anion hypothesis (1993), Singlet oxygen hypothesis (1981-1984), and Transient local heating hypothesis (1991) [30].	15
Figure 2.8	The assumed schematic representation shows predicted mitochondrial retrograde signaling pathway after absorption of laser light by cyt c molecule. Figurative representations mean: \rightarrow experimentally proved paths, dotted \rightarrow theoretically assumed paths; [] concentration; \uparrow , \downarrow increase and decrease marks. Some symbolic representations are: Δ FHH, change in mitochondrial fusion-fission homeostasis; $[\text{ROS}]_m$, mitochondria derived ROS; E_h , intracellular redox potential; Δ cAMP, change in concentration of Cyclic Adenosine Monophosphate [32].	16

Figure 2.9	Arndt-Schulz Curve depicted effects of energy density of laser light on PBM [35].	17
Figure 3.1	Summarizing the scheme of the studies.	25
Figure 3.2	Mouse fibroblast (L929) cell line cultured into 96 well-plates.	26
Figure 3.3	LHS scheme represents laser experimental set-up [36], and RHS image shows experimental equipments.	28
Figure 3.4	Representing the irradiated wells on the plate. The RHS plate displays 125 mW/cm ² and 200 mW/cm ² laser treatment irradiation; A1 and A4 were control group, the remaining was laser treatment group. On the other hand, The LHS plate was a template of 50 mW/cm ² of laser treatment. A1, A2, B1, B2 were the control group, and remaining was laser treatment groups.	29
Figure 4.1	Graph shows the results of normalized absorbance values of cell irradiated at 50 mW/cm ² with 24 h incubation post irradiation.	32
Figure 4.2	Graph shows the results of normalized absorbance values of cell irradiated at 125 mW/cm ² with 24 h incubation post irradiation.	33
Figure 4.3	Graph shows the results of normalized absorbance values of cell irradiated at 200 mW/cm ² with 24 h incubation post irradiation.	34
Figure 4.4	Graph shows the results of normalized absorbance values of cell irradiated at 50 mW/cm ² with 48 h incubation post irradiation.	35
Figure 4.5	Graph shows the results of normalized absorbance values of cell irradiated at 125 mW/cm ² with 48 h incubation post irradiation.	36
Figure 4.6	Graph shows the results of normalized absorbance values of cell irradiated at 200 mW/cm ² with 48 h incubation post irradiation.	37
Figure 4.7	Graph shows the results of normalized absorbance values of cell irradiated at 50 mW/cm ² with 72 h incubation post irradiation.	38
Figure 4.8	Graph shows the results of normalized absorbance values of cell irradiated at 125 mW/cm ² with 72 h incubation post irradiation.	39
Figure 4.9	Graph shows the results of normalized absorbance values of cell irradiated at 200 mW/cm ² with 72 h incubation post irradiation.	40

LIST OF TABLES

Table 2.1	Previous PBM studies both in vitro and in vivo.	18
Table 3.1	Experimental groups.	29
Table 3.2	Detailed parameters of laser irradiation.	30
Table 4.1	Quantitative experimental data at 50 mW/cm ² irradiation with 24 h incubation.	33
Table 4.2	Quantitative experimental data at 125 mW/cm ² irradiation with 24 h incubation.	33
Table 4.3	Quantitative experimental data at 200 mW/cm ² irradiation with 24 h incubation.	34
Table 4.4	Quantitative experimental data at 50 mW/cm ² irradiation with 48 h incubation.	35
Table 4.5	Quantitative experimental data at 125 mW/cm ² irradiation with 48 h incubation.	36
Table 4.6	Quantitative experimental data at 200 mW/cm ² irradiation with 48 h incubation.	37
Table 4.7	Quantitative experimental data at 50 mW/cm ² irradiation with 72 h incubation.	39
Table 4.8	Quantitative experimental data at 125 mW/cm ² irradiation with 72 h incubation.	40
Table 4.9	Quantitative experimental data at 200 mW/cm ² irradiation with 72 h incubation.	40
Table 4.10	The outcomes of the presented study in a nutshell. "P", "I", and "N" denote proliferative, inhibitory, and no effect on cell viability, respectively.	41

LIST OF SYMBOLS

$\Delta\Psi_m$	Mitochondrial membrane potential
ΔcAMP	Change in concentration of Cyclic Adenosine Monophosphate
ΔFHH	Change in mitochondrial fusion-fission homeostasis
$[\text{Ca}^{2+}]_i$	Calcium ion concentration in a cell
$[\text{Ca}^{2+}]_m$	Calcium ion concentration in mitochondria
E_h	Intercellular redox potential
J	Joule
J/cm^2	Energy Density
pH_i	Intercellular concentration in mitochondria
$[\text{ROS}]_m$	Mitochondria derived reactive oxygen species
W	Watt
W/cm^2	Power Density

LIST OF ABBREVIATIONS

3T3	Murine Fibroblast Cell Line
AP - 1	Activator Protein
ATP	Adenosine Triphosphate
ANOVA	Analysis of Variance
CCD - 1064SK	Human Epithelial Fibroblast Cell Line
COX or Cyt c	Cytochrome C Oxidase
cAMP	Cyclic Adenosine Monophosphate
CW	Continuous Wave
DMEM	Dulbecco's Modified Eagle's Medium
DMSO	Dimethyl Sulfoxide
EMR	Electro Magnetic Radiation
ECT	Electron Transport Chain
FBS	Fatal Bovine Serum
IR	Infrared
L929	Murine Fibroblast Cell Line
LHS	Left Hand Side
LLLT	Low Level Laser Therapy
MTT	3-(4,5-Dimethyliazol-2-yl)-2,5 diphenyltetrazolium bromide)
NIR	Near Infrared
NO	Nitric Oxide
NF- κ B	Nuclear Factor κ -B
PBM	Photobiomodulation
PDT	Photodynamic Therapy
PBS	Phosphate Buffered Saline
ROS	Reactive Oxygen Species
RHS	Right Hand Side
SPSS	Statistical Package for the Social Sciences
TNF- α	Tumor Necrosis Factor Alpha

UV	Ultraviolet
WS 1	Human Skin Fibroblast Cell Line
VIS	Visible



1. INTRODUCTION

1.1 Motivation

Medical lasers have been used in surgical operations and applications such as cutting, ablating, removing the tissue since 60s. First medical laser laboratory was launched in the University of Cincinnati, since then scientists have developed the many different functions of the lasers in medical sciences. Laser therapy is also a non-invasive therapeutic procedure in which laser light energy repairs and regenerates damaged skin. [1, 2]. Since the potential risks have reduced in laser light due to low power irradiation, researchers and companies in this sector have tried to enhance healing characteristics of laser light in a new area differ widely than existing treatments [2].

Photobiomodulation, known as low level laser therapy (LLLT), is a method which affects on a cell or tissue response due to low intensity laser interaction without heating effect. Low power lasers can be utilized for increasing in number of cell and decreasing in senescence of fibroblasts [2].

When a photon interacts with a cell or tissue, the photon becomes an energy packet which stimulates a cell or a tissue. If irradiation time is increased, since more photons are emitted the more energy is taken; therefore more stimulation occurs. The stated biostimulatory response is dose dependent; in other words, it has a therapeutic window. Unless electromagnetic wave radiation is applied in the range of optimal parameters, the stimulatory effect disappears or turns into inhibitory form [3].

Jerkins and Carroll (2011) reported that there are some important parameters of laser light: wavelength, power, energy, irradiation time, beam area (spot size), power and energy densities, irradiation mode (i.e. pulsed or continuous wave (CW) etc. Moreover, numbers of treatments, interval between the laser applications might also change the efficacy of the application [4].

The methods performed in the previous studies, asserted in Chow's research (2000), correspond to each other, even though they can lead to different outcomes like activating or deactivating cell metabolism. Therefore, selecting the proper irradiation dose, and the accurate methodology, and reporting them in details are very critical, which clarifies and guides the latter studies [5].

Jerkins and Carroll (2011), and Chow (2000) addressed that majority of published studies about PBM do not indicate whole beam parameters or dose information mentioned above. Power density of laser light is one of the omitted parameter that should be declared. In some previous studies, researchers have preferred to use parameters such as wavelengths, energy densities as similar to their colleagues. Particularly, energy densities ranging 1-4 J/cm² are the gold standard of biostimulation which is used in many researches; however, although the same parameters are used, the outcomes might show very different effects [4, 5]. We have no evidence to refer proper parameters due to lack of information on beam parameters of dose information mentioned above.

In this study the main question is the impact of power density on the efficacy of proliferation and viability of mouse fibroblast cells in vitro. Detailed presented research tries to provide and determine the upper and lower threshold values of effective power density; this would clarify whether the incubation interval alters to the proliferation rate of cells in vitro after the laser treatment.

1.2 Objectives

The purpose of the presented study is to understand the effectiveness of PBM on murine fibroblasts in vitro in terms of varied laser dose, power density, and incubation intervals post irradiation. The detailed aims mentioned below are considered in this conducted research:

- To investigate the effect of visible laser (635 nm) at different power densities on

cellular response of L929 cell line,

- To define the effective minimal and maximal limits of power density values for successful treatment to increase proliferation rate in vitro,
- To determine the best incubation time interval for better proliferation after the laser treatment in vitro,
- To understand whether an adverse long term effect of laser treatment might be possible in vitro.

1.3 Outline

Chapter 1, the introduction, covers the motivation and objective of the research are stated.

Chapter 2 includes background information on fibroblast morphology and characteristics, cell proliferation, laser - tissue interactions: absorption, scattering and penetration of light in tissue, photochemical effect of interaction between laser and tissue, photobiomodulation: its history, mechanism, and critical parameters in literature.

In Chapter 3, all experimental design and protocols of the study are explained.

Chapter 4 gives and discusses the results of the experiments conducted for the study, and analyses the efficacy of the parameters presented by comparing with previous studies.

In Chapter 5, the results of the research are concluded.

2. BACKGROUND

2.1 Fibroblast Cells

The coverage organ, skin, is the largest organ of the body. Skin is obtained from the mesoderm lineage and contains two distinct layers: loose and superficial papillary layer which is waver, and deeper and reticular denser layer. Skin is comprised epidermis, and dermis that is the inner layer and placed under the epidermis. Fibroblasts, macrophages, plasma cells, mast cells, and some components of connective tissue exist in papillary layer [6].

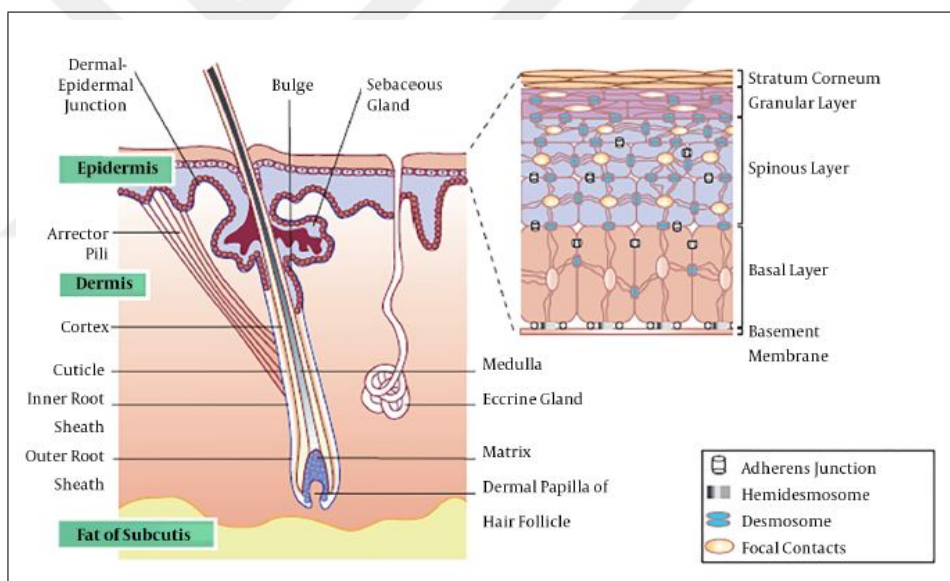


Figure 2.1 Illustration of dermatological layers and components of the skin [6].

Fibroblasts are very important cell types since it has high survival and proliferation rate [6]. Dermal fibroblasts which are heterogeneous and highly dynamic cell line consist of local extra cellular matrix which supports cell survival, and proliferation. Fibroblasts vary according to different tissue types, and even alter its morphology regarding the tissue type where the cells exist. It is also benchmark of cutaneous wound healing [7].

Fibroblasts are consisted great amount of connective tissues. They contribute to strengthen structural condition in the tissue [6]. Fibroblasts, motile with bundles, have elongated body shape [8]. They occupy spaces with substratum therefore no other fibroblast cells can take place. If a fibroblast touches another fibroblast, instead of a temporary adhesion, they create a meshwork of adhering cells.

Fibroblasts, in vitro, can multiply themselves easily. They can disregard the limitations and rules of cell cycle. They might be able to divide infrequently, thereby the cell population reaches to high numbers. In the same cell culture, both high density and low density of cell population can be seen in the different areas, which might result from some changeable conditions and environmental factors affecting on stopping feedback mechanism of cell cycle [9]. Overall, in vitro proliferation rate of fibroblasts does not depend on only its natural cycle, but the other environmental factors such as incubation time, incubation temperature, and nutritional supply of culture medium.

2.2 Cell Proliferation

Growth factor regulates cell proliferation by converting signals in order to advance into beginning of cell cycle. Cell proliferation generates two distinct cells from one cell as a result of cell growth. In body of a living multi-cellular creature, a large number of cells proliferate, as long as the system allows them continuing this process. Under the standard circumstances, proliferation rate is controlled by regenerative cells of the tissue [10].

Tissues, which are organized into organs, are formed by enormous populations of cells, total more than 10^{14} . Surprisingly, mortality rate of cells reaches approximately 10^{12} cells in a day so that body sustains its life. Some cell types like skin and bone marrow can proliferate during their lifetime; contrarily, the some other ones like bone and muscle cells stop active cell division, in adulthood period [11].

Majority of normal cells, which have proliferative characteristics, grow, to replace death or damaged cells. When this mechanism starts to act out of its natural regulation, impaired cell cycle causes over proliferation, which leads to extreme accumulation of cells. If this abnormally self-divide continues, the malignant character can be passed on to the daughter cell and the granddaughter cells as well. This abnormal situation might be a sign of a cancer [12].

Animal cells are classified into different groups with respect to characteristics of proliferation. One type of cells can never be produced in case of an injury. For instance, when a person suffers from heart attack, cardiac muscle cells dies, and remaining cells cannot proliferate. Another type of animal cells keeps proliferation sustainable even if the cell enters the G0 (inactive state), because it needs to replace cells in case of cell death or injury. Some examples of this type are, skin fibroblasts, smooth muscle cells, and endothelial cells which align with the inner surface of blood vessels, and cover internal organs like liver, pancreas, kidney, lung, prostate, and breast. In case of cutaneous wound, skin fibroblasts repair the injury with rapid proliferation. Liver tissues are a good example of rapid proliferation. In normal conditions liver cells divide infrequently; however, when excessive amount of cells are lost due to surgery, remaining cells starts to proliferate to regenerate new cells in the place of removed tissue. The other type of cells have limited period of time to live under normal conditions. They cannot proliferate, when they are fully differentiated. Instead of proliferating themselves, they are replaced by less differentiated cells [13].

If the tissue is wounded, cells enhance a unique pathway as a healing process. This process comprises distinct and overlapping phases, such as inflammation, proliferation, and remodeling. The first stage is inflammation. In couple of days, injured area might be occupied by inflammatory neutrophils and cytokines, particularly tumor necrosis factor alpha (TNF- α) which are responsible for activating keratinocytes, macrophages and fibroblasts. Tumor necrosis factor alpha plays important role in expression of growth factors in order to accommodate angiogenesis and collagen synthesis. The next phase is proliferative phase, and takes place in between 5 to 14 days. During this phase, many activities realized such as vascular endothelial formation, extracellu-

lar matrix formation, and re-epithelization. The last phase is remodeling, starts on day 21. It might take months, depending on extent and depth of the scar. Remodeling is the maturation part of covalent bonds between the molecules. In this phase collagens are remodeled, and fibers become thicker, stronger and more organized.

Natural wound healing process might not be sufficient enough for the healing process. Therefore, if necessary, it can be supported by PBM to regenerate cutaneous lesions and accelerating healing [14].

If tissue is wounded, cells are prone to closure. This natural tendency is as result of cellular behavior, migration or proliferation. Cell population rate, incubating time, inhibitory chemicals of cell proliferation, lack of serum in the medium have impact on cellular behavior [15]. Consequently, increase or decrease in proliferation rate can be result of other conditions which should also be considered about.

2.3 Laser-Tissue Interactions

LASER is an acronym of "Light Amplification by Stimulated Emission of Radiation". It emits intense electromagnetic radiation due to its narrow beam and condensed energy. Emitted photons have constant phase difference; they are in the same frequency; they have the same waveform. As a result of these similarities, Laser light is coherent. The light generates photons which have the same wavelength with each other (i.e. monochromatic light). There are various laser types, and the material that make laser irradiate can change its characteristic. They can be gases, crystalline solids, polymers and etc. Regarding their design, some lasers produce continuous beam, and pulsed beam emitting rapid and ultra-short pulses. By adjusting the laser parameters, they can be utilized in various areas. Among laser applications, medical laser applications are one of the most common areas. Medical lasers can lessen blood loss, reduce pain, seal blood vessels, stop bleeding of ulcers, destroy tumor cells, and accelerate wound closure etc.

The fundamental interaction mechanism of laser-tissue interactions mainly is related to absorption and scattering of coming photons [16]. An atom or a molecule, apart from exceptional ones, has many electronic states. When a photon hits an atom, it can be absorbed or scattered depending on its energy (i.e., $E = h\nu$) due to the result of the interaction between them. The primer effect of photostimulation in the cellular level results of light absorption that induces transition between the states can be either radiative or non-radiative [17]. The photon absorption depends on the characteristics of the target molecule (i.e. chromophore) that absorbs the photon at a particular wavelength. The chromophores (i.e. tissue absorbers, or target molecules of specific range of wavelength) such as water, lipids, melanin, oxy- and deoxyhemoglobin etc. have absorbance spectrum in the range of UV-VIS-IR. Tissues have various chromophores and some of them represented in Figure 2.2, but only the predominant ones determine the optical absorption within the layer. Absorption leads to photothermal and photochemical effects and subsequent chain of photobiological reactions [18].

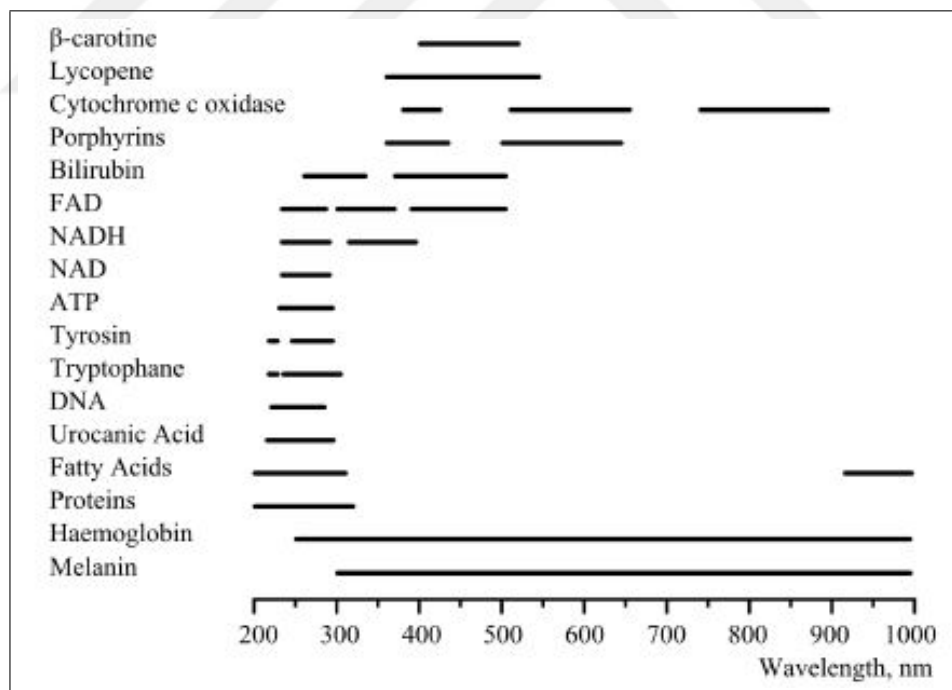


Figure 2.2 Representation of photospectral range of main tissue absorbers of human skin and other tissue types [18].

If the energy of incident atom and the energy between the excited state and the current state of the atom are consistent with each other, the photon is absorbed

by an atom. The released energy is transferred to thermal energy and random atomic motions by the collisions. Then, the photon whose energy is less than incident one is emitted. Thus, the entire process is called absorption. When a molecule absorbs energy from electromagnetic radiation (EMR), a number of directions are followed, and finally it goes back to its ground state, which is schemed in Jablonski diagram, Figure 2.3 [17].

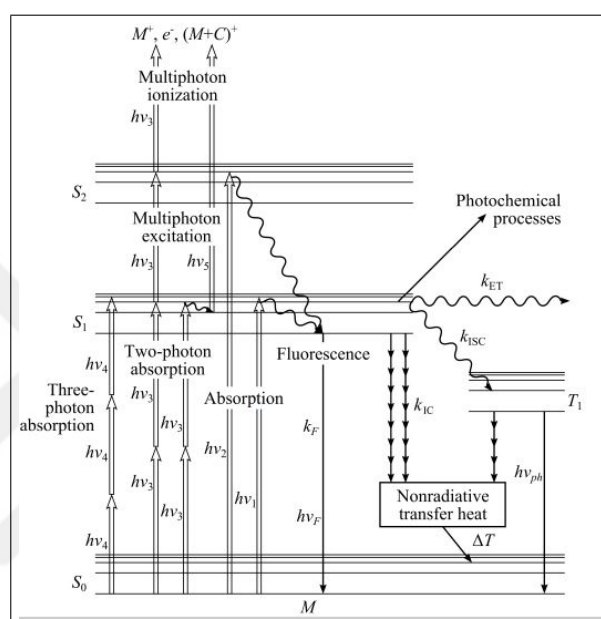


Figure 2.3 The scheme which is Jablonski diagram of molecular energy levels of excitation, ionization, and relaxation shows principle of the light interaction with M molecule. The transition rates are indicated by straight lines which are radiative transition; waving and multi arrow lines are non-radiative [19].

The other main interaction type is scattering which can be elastic, or inelastic. If the scattered photon has different frequency from the frequency of the incident atom, it is called as inelastic scattering. The scattering of small fraction of the light might result from excitation of an atom. Raman scattering is an example of inelastic scattering. On the other hand, as long as the scattered photon has the same frequency and wavelength with the incident photon, it is named as elastic scattering. One of the most known elastic scattering types is Rayleigh scattering. The scattering center might be subcellular components, and organelles, etc. Three parameters affect on this type of scattering; the size of scattering center, refractive index difference between the scattering center and surrounding medium, and the wavelength of light. Consequently, shorter wavelengths (i.e. blue lights) tend to scattering more than longer ones (i.e. red

lights). In addition, the longer wavelength of light brings about deeper penetration. However, it has a limit. The upper limit of the wavelength is in the IR range where absorption of light is occurred by water [17].

A biological tissue which has a refractive index greater than air's is one of a dielectric medium. Consequently, if a photon interacts with a tissue, it might cause a partial reflection since having an interface between two surfaces, tissue and air; the remnant part might pass through the tissue [18].

Due to absorption and scattering characteristics of light, it can penetrate in tissue. When light propagates in the medium, it causes in spatial variations due to the refractive index of the medium [20]. Higher energy absorption results in the less depth of penetration of the light. Thus, shorter wavelengths (200-600 nm) travel on the surface; on the other hand, longer wavelengths (650-1200 nm) can penetrate deeper [21].

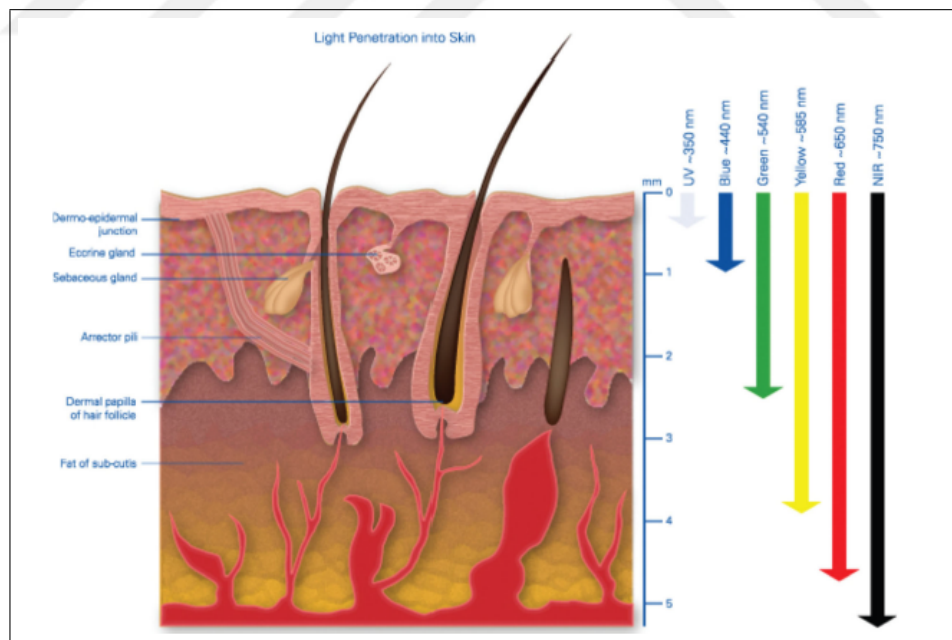


Figure 2.4 Graphical representation of how light penetration is changed by wavelength [22].

According to Ash et al., penetration of light in tissue increases with wavelength. For multi-layer skin model, ultra violet (UV), visible (VIS), and near infrared (NIR)

radiations were designed via Monte Carlo Simulation. According to the observations, maximum penetration was measured as $5378 \mu m$ with computational methods. In addition, penetration depth was affected by spot size, and larger spot size increases penetration depth of the light. Overall, laser geometry and wavelength of light influenced on penetration of light.

Wavelengths of red range pass through more distance in skin layers than wavelengths of blue range due to the absorption range of the chromophores and scattering coefficient of the molecules. It is very crucial that incident photon should target the chromophores. Thus, preference of the wavelength determines penetration depth which affects on absorption of incident light; if there is no absorption, there can be no reaction [22].

Power [W] and spot size [cm^2] are also important parameters of laser light to control the penetration mechanism. The two parameters give power density which determines how much energy and heat targets to the specimen. If beam radius (i.e. spot size, or beam width) is decreases, power density will be increased. The narrow spot size results in decreasing in the treatment area, due to lower penetration depth, which affects on sudden scattering of the photons under the tissue layer. In other words, beam radius should not be smaller than penetration depth; otherwise, irradiation energy of the light on the tissue is become decreased [21].

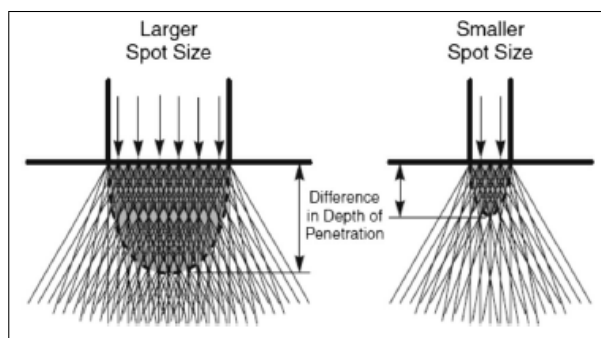


Figure 2.5 Representation of effect of beam width on light penetration [22].

2.4 Photochemical Effect of Interaction between Tissue and Light

Light can stimulate chemical reactions in macromolecules and tissues. Interaction between matter and light causes chemical modifications which called as photochemistry. Photochemical system consists of light as a reactant [23, 24]. When photons are absorbed by target molecules, they are excited to upper energy states. If the molecules are leveled down to lower energy states, the released energy is utilized to produce some high energy species which tend to be reactive to surrounding molecules, target molecules. In addition, there might be a third component such as photosensitizer, photoinhibitor, or photocrosslinker, etc. [25].

In the photochemical interaction, there are two main types of applications: Photodynamic therapy (PDT), Photobiomodulation (PBM).

Considering PDT, photosensitizers destroy malignant tumors and diseases with activation of light. It absorbs specific wavelengths of the light; after the absorption, the mechanism of generation of reactive oxygen species (ROS) are triggered, which causes necrosis of photosensitizer applied cells or tissues [17].

For low level laser interaction with living tissue, photons have effects on cell proliferation. Various studies about wound healing treated by PBM were published. In addition to accelerating healing process, the previous investigations comprised the studies of pain relief, reduction of inflammation, and tissue regeneration etc. [26]. In terms of therapeutic characteristic of PBM, the irradiation dose of laser light induces cellular reactions taking place in mitochondria. However, there is no consensus of optimal doses; therefore, PBM applications are required more detailed exploratory researches.

2.5 Photobiomodulation (PBM)

PBM is irradiated between red and NIR wavelength to promote healing process, lower inflammation infiltrate, and reduce pain. PBM technique is developed by Endre Mester over 50 years ago. Various wavelengths in the red range of VIS, 600-700 nm, and NIR, 770-1200 nm, spectrum have supportive results for better stimulation of cell biochemical reactions. However, laser applications at the region of 700-770 nm have limited positive biochemical outcomes. Maximum limit of NIR wavelengths is 810 nm; above this wavelength water becomes a target chromophore which is primer absorber [27].

Mitochondria play a critical role in cellular interaction of light since mitochondria consist of majority of biomolecules and other cellular structures such as cytochrome c oxidase (cyt c, or COX), some proteins, nucleic acids, and adenine nucleotides etc. They are quite essential molecules of biochemical reactions. In addition, the major cell chromophores, flavins, iron-sulfur centers, and heme, are also found in mitochondria. Thus, mitochondria are the critical component of light - cell interactions [28]. Meanwhile, mitochondria are both responsible for energy production and cell regulations including signaling and cell death.

Cyt c, a photo-acceptor, is the one of the four enzyme complexes which is generated by mitochondrial electron transport chain (ECT), and is responsible for transferring electrons from the donor molecule to the acceptor molecule across to inner mitochondria. Presumably, energy of the photon is absorbed by cyt c that has several metal sites containing to hemes ("a" and "a₃") and two copper centers (CuA and CuB), which cause visible light absorption [29]. The mechanism of PBM depends on the electronic excitation of the copper centers in cyt c molecule.

The mechanism is a two-step action: primary reactions and secondary reactions. The primary reactions introduce the secondary reactions which are photo-signal transduction chain in mitochondria. Secondary reactions take place, after laser irradiation stops [30].

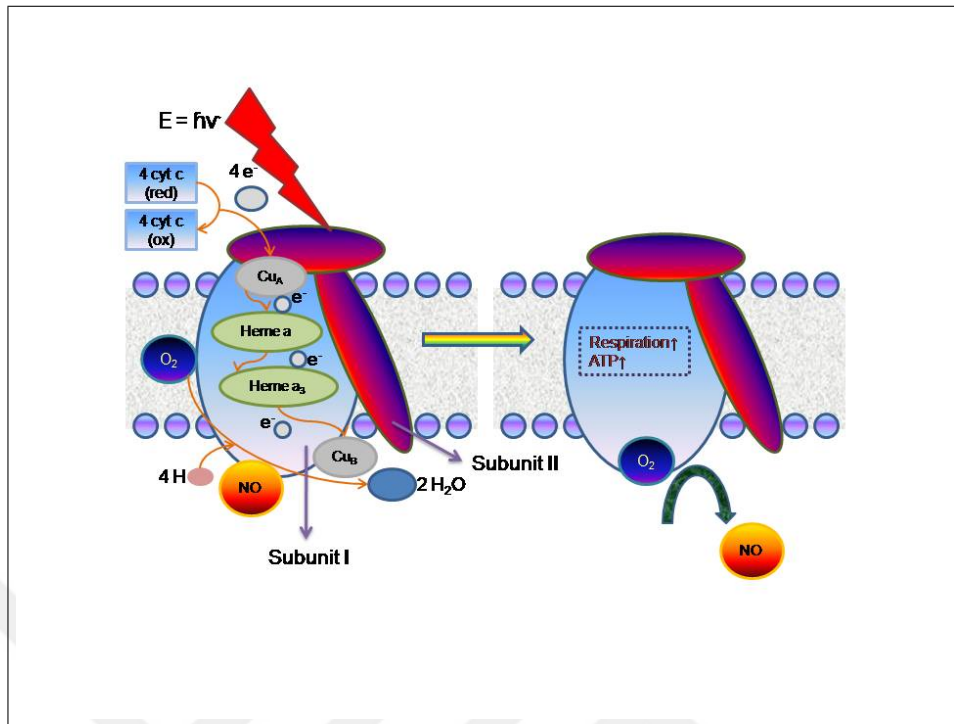


Figure 2.6 The scheme of interaction between laser light and cyt c molecule.

The flow of electron transfer between $\text{Cu}_A \rightarrow \text{heme a} \rightarrow [\text{heme a}_3 - \text{Cu}_B]$ catalytic center $\rightarrow \text{O}_2$ is suddenly occurred within cyt c molecule [30].

If mitochondria are under stressed, or oxygen level, nitric oxide (NO) is generated and interferes with respiration, since NO and O_2 counteract each other. Due to photo-induced interactions in cyt c molecule, PBM raises the NO concentration that arises from the redox reaction. As a consequence of respiration chain, NO connects with cyt c; therefore, restoration of O_2 restarts respiration, which causes ROS production. ROS have key role for adenosine triphosphate (ATP) production that supplies energy to the cell.

PBM leads to reestablishing respiratory reactions via releasing NO by iron ions and copper centers of cyt c; increases in oxygen recapture level, and stimulates production of ROS and ATP. Moreover, PBM also encourages DNA and RNA transcription factors. PBM action depends on the increase in ROS level which produces hydroperoxide anion, and induces hydrogen peroxide (H_2O_2). These alterations have impact on transcription factors such as primarily Nuclear Factor κ -B (NF- κ B) and Activator

Protein 1 (AP-1). Thus, production of ROS has an important role for both intracellular signaling and advancement of nucleic acid synthesis in the nucleus. Furthermore, PBM triggers intracellular Ca^{2+} ions which encourage DNA and RNA synthesis and increasing in cell proliferation [31].

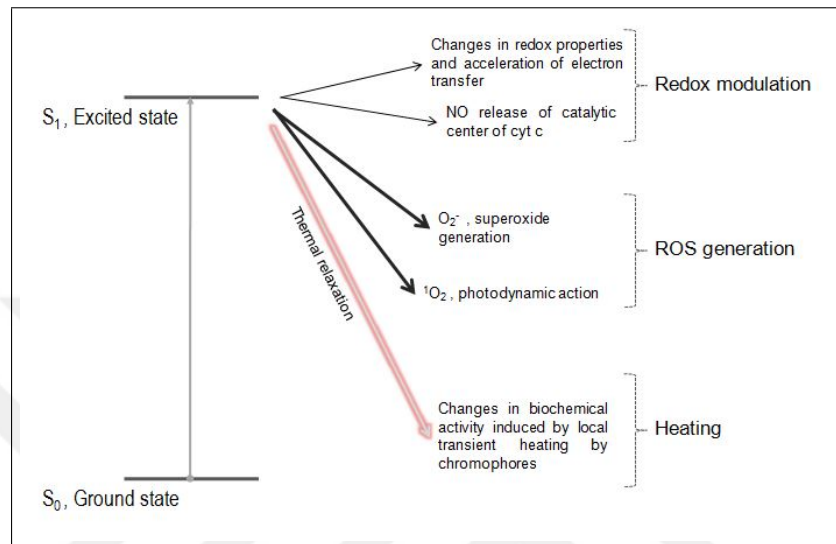


Figure 2.7 Assumed primary reactions in COX molecule after excitation of an atom from the ground state to the upper energy states. S_1 is only figurative state, not obligatory. These are the hypothesis of Karu's studies: Redox properties alteration hypothesis (1998), NO hypothesis (2005), Superoxide anion hypothesis (1993), Singlet oxygen hypothesis (1981-1984), and Transient local heating hypothesis (1991) [30].

Cell proliferation model is one of the results of mitochondrial retrograde signaling shown in Figure 2.8, and is a proof of the existence of communication chain between mitochondria and rest of the cell. Mitochondrial membrane potential ($\Delta\Psi_m$), ROS, Ca^{2+} concentration in a cell ($[\text{Ca}^{2+}]_i$) and in mitochondria ($[\text{Ca}^{2+}]_m$), free radical NO^\cdot , intracellular pH (pH_i) and parameters related with mitochondrial biogenesis are influenced by the signaling pathway [32].

The stage of mitochondrial retrograde signaling pathway is recognized as a secondary reaction of PBM since the outcomes of the reactions occur after the laser irradiation. Essentially, the sudden reactions happen along with absorption of light by cyt c are defined as primary reactions; and subsequent photosignal transductions are defined as secondary reactions. In other words, secondary reactions include photobiological responses [33].

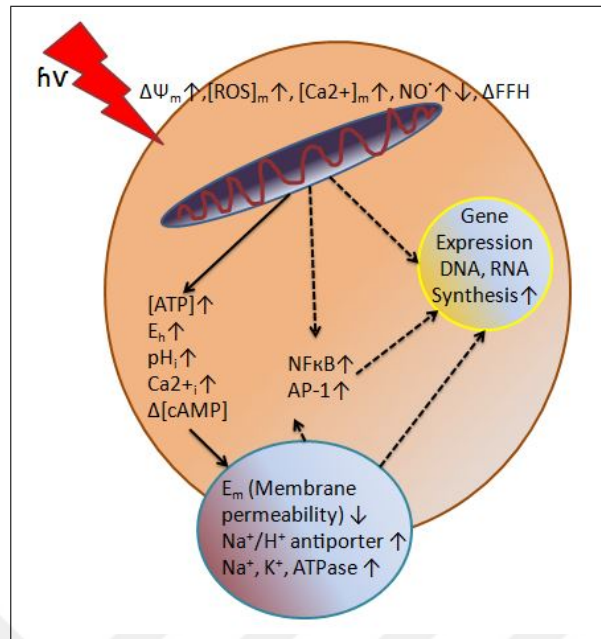


Figure 2.8 The assumed schematic representation shows predicted mitochondrial retrograde signaling pathway after absorption of laser light by cyt c molecule. Figurative representations mean: \rightarrow experimentally proved paths, dotted \rightarrow theoretically assumed paths; [] concentration; \uparrow , \downarrow increase and decrease marks. Some symbolic representations are: ΔFFH , change in mitochondrial fusion-fission homeostasis; $[\text{ROS}]_m$, mitochondria derived ROS; E_h , intracellular redox potential; ΔcAMP , change in concentration of Cyclic Adenosine Monophosphate [32].

Intensity and dose of laser light have effects on the metabolic activity of mitochondria cyclic changes. Characteristics of the stimulations depend on the threshold values. Either exceeding maximum limits or falling behind the minimum limits might generate inhibitory responses in the cellular mechanism, because irradiated light characteristics links to cellular signaling pathways including mitochondrial retrograde signaling [32].

PBM efficiency depends on wavelength, irradiance, laser duration time, operation type (like continuous wave, or pulsed etc.), polarization of light, coherence, cell type in vitro. Output power of laser light varies between 1-1000 mW regarding the type of the treatment. Efficacy of PBM applications depends mainly on different parameters of energy and power density. In addition, deciding on optimum dose is a puzzling situation. Therefore, most of the time parameters are selected by data of literature and personal choice or experiences of the researchers [34].

PBM defines the biphasic dose. When the dose used is between recommended values, response of treatment increases the efficacy. However, if it is used beyond the maximum value, positive effect of the treatment reduces. Eventually, the stimulatory influence turns into inhibitory effects, and finally it vanishes [27].

The biphasic response is known as Arndt-Schulz Law. Hugo Schulz had published his study in 1887, expressing several low doses effects on the yeast metabolism. When he collaborated with Rudolph Arndt, they discovered that using low doses stimulate the activity until it reaches the maximum dose. When maximum dose is exceeded, cell activity decreases [34].

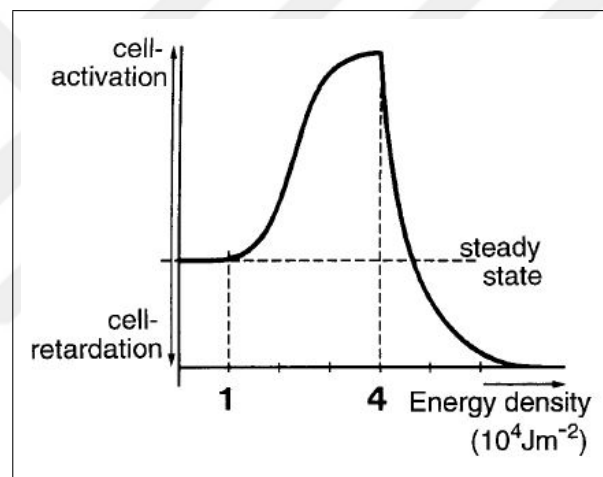


Figure 2.9 Arndt-Schulz Curve depicted effects of energy density of laser light on PBM [35].

Due to the biphasic dose response to PBM, low doses are prone to improving the activity of cell metabolism. According to researchers in literature, PBM applications are popular in dermatology, dentistry, rheumatology, physiotherapy. The major purposes of low power laser treatment are stimulating wound healing, healing bone fractures, tendon ruptures, spinal cord injuries, traumatic brain injuries, heart attacks, stroke, and relieving pain, inflammation, edema [34].

Many studies based on the molecular and the cellular mechanisms, including the photons that are absorbed by the mitochondria, ATP and ROS production, activation of transcription factors.

Table 2.1
Previous PBM studies both in vitro and in vivo.

Author	Treatment	Results
Solmaz et al., 2017 [36]	<p>Mouse fibroblast cells were irradiated with 635 nm and 809 nm, separately. Energy densities of irradiation were 1 J/cm² and 3 J/cm²; output power was 50 mW. Viabilities of cells were measured at 24th, 48th, 72nd hours to analyze cell activity. Similarly, 24 rats were exposed to same treatment procedure regarding the laser parameters. The treatment was applied to each dorsal cutaneous wound of the rats. Wounds were examined on day 3, 5, and 7, respectively.</p>	<p>For both energy densities of 635 nm had proliferative effects in terms of MTT results, after 24 h incubation post laser irradiation. With respect to the incubation interval of 72 h, 1 J/cm² enhanced the proliferation effect. For in-vivo experiments, 635 nm stimulated wound healing with both energy densities. Laser irradiation at 809 nm had no effect on cell proliferation neither positively nor negatively for both in-vitro and in-vivo study.</p>
Serdari et al., 2016 [37]	<p>HeNe laser (i.e. 632.8 nm) irradiation at 1 J/cm² was applied to lesions of Buccal mucosa on 32 rats. Laser treatments were applied to the defined groups on the day 1, day 1 and 2, and combination of day 1 and day 3.</p>	<p>There was no significant difference between the laser treatment group and the control groups. However, wound closure was in good form at the end of the third day compared to the other treatment intervals.</p>
Lau et al., 2015 [38]	<p>6mm dorsal diabetic wounds on rats were irradiated with 808 nm laser light whose intensity were 0.1 W/cm², 0.2 W/cm², 0.3 W/cm².</p>	<p>Laser treatment increased the closure of the wounded area compared to healing progress of non-irradiated group; regarding the results, the most efficient optimal parameter was 0.1 W/cm².</p>

Author	Treatment	Results
Marques et al., 2014 [39]	<p>L929 (mouse fibroblast) cell line was cultured in 5% and 10% supplemented FBS (fetal bovine serum), separately. The cultured cells were irradiated with 685 and 830 nm laser light to observe the responses on them. Laser energy densities were ranged in 0.1 - 30 J/cm² (i.e. 0.1, 0.5, 1, 2, 3, 5, 7, 10, 20, and 30 J/cm²) to understand the efficacy of PBM effect.</p>	<p>There was no remarkable results in the treated cell line cultured in 10% FBS. On the other hands, cells in 5% FBS medium were stimulated by 5 to 30 J/cm² of energy densities; contrarily, 0.1 to 3 J/cm² of laser energy density caused suppressive effect on cell proliferation.</p>
Kilik et al., 2014 [40]	<p>48 rats, grouped as diabetic and non-diabetic, were exposed to surgical wounds. The treatment was occurred with 635 nm laser three times daily. The selected doses were 1, 5, 15 mW/cm². For the analysis, experimental samples were euthanized on day 2, 6, and 14</p>	<p>Polymorphonuclear leukocyte infiltration was decreased by 15 mW/cm² of power density. 5 mW/cm² and 15 mW/cm² increased the amount of collagen fibres compared to the other groups in non-diabetic rats. In diabetic group, significant difference was occurred at the power density of 15 mW/cm² regarding the ratio of Polymorphonuclear leukocyte/Macrophages. Formations of new capillaries were significantly increased by irradiation at 5 mW/cm² and 15 mW/cm² on day 6 in comparison with the control group.</p>

Author	Treatment	Results
Esmacelinejad et al., 2013 [41]	Regarding glucose concentration of the growth medium, human skin fibroblasts were grouped. Applied doses were 0.5, 1, and 2 J/cm ² with a constant power density as 0.66 mW/cm ² and 632.8 nm. The laser was treated the cells three consecutive days.	At 0.5 and 1 J/cm ² , human skin fibroblasts cultured in physiologic glucose medium enhances the proliferation stage as compared to control group. The irradiated groups stimulated the proliferation rate of Human Skin Fibroblast in high glucose concentration.
Basso et al., 2012 [42]	Gingival fibroblast cell culture was irradiated with 780±3 nm and 40 mw output power. Fluence of the irradiation was 0.5, 1.5, 3, 5, 7 J/cm ² , separately. Cells were treated for three following days without any examination.	Cell metabolism was significantly enhanced by laser light exposure at 0.5 J/cm ² and 3 J/cm ² compared to the control group. There was no statistically significant difference between 5 J/cm ² and other treatment groups. 1.5 J/cm ² and 7 J/cm ² treatments had negative impact on cell viability in comparison with the control group.
Lacjakova et al., 2010 [43]	The conducted in-vivo study included two groups, non-steroid and steroid treated. Each rat had four surgical dorsal wound. The laser treatment was performed with 670 nm. Applied laser dose was 5 J/cm ² of energy density. The treatment was performed daily, and the treatment interval was six days. The experimental groups were determined according to power density value (i.e. 5, 15, 40 mW/cm ²).	Inflammation rate of non-steroid group was decreased significantly by the treatment with 40 mW/cm ² of power density. 15 mW/cm ² and 40 mW/cm ² raised proliferation rate of fibroblast cells significantly. However, there was no remarkable difference between the steroid-treated rats.

Author	Treatment	Results
Busnardo et al., 2010 [44]	HeNe laser was applied to wound area with 4 J/cm ² of fluence for 12 sec. Laser beam area (i.e. 0.015 cm ²) was irradiated with 5 mW output power.	Wound inflammation was decreased. In addition, laser irradiation also increased type III collagen synthesis.
Silva et al., 2010 [44]	15 rats were divided into three groups: control, and laser treatment groups (i.e. 2 J/cm ² , and 4 J/cm ²). Laser light at 670 nm was used for treatment during 10 following days.	4 J/cm ² of energy density caused significant difference in re-epithelization process comparison with the other groups.
Maiya et al., 2009 [44]	Skin wound of diabetic rats were treated by HeNe laser light with the dose between 3-9 J/cm ² for five days/week. The treatment was continued until wounds healed.	In fifth days, 4-5 J/cm ² laser energy densities increased generation of granulation of tissue.
Gal et al., 2009 [45]	Experimental subjects were divided into two groups: non-steroid laser treated and steroid treated groups, separately. The wounds were subjected to 635 nm laser light. Applied power density values were defined the experimental groups (i.e. 1, 5, 15 mW/cm ²). Rats were euthanized on day 2, 6, and 14 to observe the effect of the treatments.	The epithelization and collagen synthesis on the day 2 and 6 in non-steroid groups. In steroid laser treated group of rats, the laser treatment decreased the leukocyte/macrophage ratio, and granulation of tissue.

Author	Treatment	Results
Inoe et al., 2008 [44]	Healthy rabbits were exposed to HeNe laser light with output power 45 W. Experimental groups were irradiated by 3 and 6 J/cm ² of energy densities, separately. Analysis of the experiments was evaluated on day 7, 14, and 21.	According to the results acquired on day 14, laser treatment reduced the hemorrhage and oozing of the body fluid; in addition, the mature granulation of tissue was also observed on the same day.
Rocha et al., 2007 [44]	12 experimental samples were divided into 2 groups; control and laser treated. The dose of pulsed laser was 3.8 J/cm ² with the output power of 15 mW. The treatments were occurred for 7 days.	In the experimental group, wound contraction was accelerated by laser treatment.
Demidova-Rice et al., 2007 [46]	The mice having surgical dorsal wounds were irradiated with 635±15 nm non-coherent light source to comprehend cellular response to the dose. Treatments were applied once. The defined laser fluences are 1, 2, 10, and 50 J/cm ² . Applied power densities were ranged in between 80-100 mW/cm ² .	Fluence of 1, 2, 10 J/cm ² had positive impact on wound closure. However, the most efficient fluence was 2 J/cm ² . On the contrary, energy density of 50 J/cm ² caused suppressive effect on healing process.
Hawkins et al., 2006 [47]	HeNe laser was applied to human wounded fibroblasts for two consecutive days. Different treatment groups were irradiated with 0.5, 2.5, 5, 10, 16 J/cm ² , respectively.	Applied dose of 5 J/cm ² increased cell viability. On the other hand, higher doses reduced cell proliferation, and they were significantly harmful for the cell membrane and DNA.

Author	Treatment	Results
Kreisler et al., 2003 [48]	Periodontal ligament fibroblast cells were exposed to 809 nm laser light. The treatments were applied for three days. Observations were done at the end of each 24 h. Treatment doses were defined as 1.96, 3.92, and 7.84 J/cm ² .	Laser treated groups caused significant proliferation rate than control group. 24 h and 48 h incubation post irradiation had remarkably increased cell proliferation. However, 72 h incubation post illumination reduced cell viability moderately.
Pereira et al., 2002 [49]	904 nm (with output power 120 mW) and the energy densities of 3 to 5 J/cm ² laser light illuminated embryonic murine fibroblasts for 6 days.	3 and 4 J/cm ² laser doses activated cellular metabolism for proliferation. On the other hand, 5 J/cm ² had no significant impact on proliferation and pro-collagen synthesis.
Envemeka et al., 2001 [50]	Cutaneous wounds of calcaneal tendon in each rabbit were performed. The wounds were irradiated by two different laser sources, HeNe (i.e. 632.8 nm with 11 mW output power) and Ga:Ar (i.e. 904 nm with 7 mW output power).	Both these two different wavelengths were efficient for wound healing. However, depends on the tissue type, penetration depth of laser light might change.

Table 2.1 summarizes the previous studies of cell proliferation of fibroblasts and wound healing processes both in vivo and in vitro. PBM is a familiar application to stimulate cellular and molecular mechanism in variety system of our body. Unfortunately, the optimal parameters and the limits of efficient parameters are not clear.

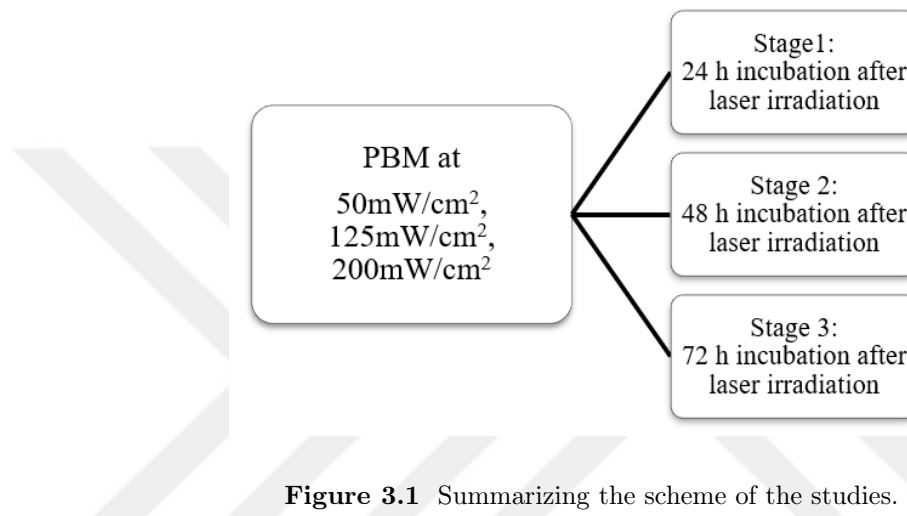
According to Kara et al. (2017), PBM can increase the survival rate of existing cancer cells and their proliferation rate. However, there is no study has certainly proven yet whether potential cancer cell might transformed into cancer cells by PBM treatments [51].

Consequently, the goal of the study is to define the limits of power density that regulate the treatment effect properly and to analyze the short and long term effects of radiation on cell basis.



3. MATERIALS AND METHODS

The presented study is divided into three separate stages as given Figure 3. In each stage, the same procedures except for incubation interval post irradiation are used.



3.1 Cell Culture

L929 (mouse fibroblast) cells were obtained from the Biomaterials Laboratory of Institute of Biomedical Engineering at Boğaziçi University. Complete grown media which as Dulbecco's Modified Eagle's medium (DMEM) at 37°C was supplemented by 10 % fetal bovine serum (FBS, Gibco) and %1 antibiotic-antimycotic solution (Sigma).

When cells were thawed, growth medium was warmed in 37°C water bath before starting. Cryovial tube was placed inside the warm water bath for several minutes until a very small ice crystals remaining. Cryovial content was transferred inside a centrifuge tube. 3 ml complete medium was added into the tube, and cells were spun at 1000 rpm for 5 min. After the centrifuge process the supernatant fluid was aspirated by pipette. 5 ml complete medium was added over the cell pellet and cells were dispersed gently.

Cells suspension was transferred into T25 flask carefully. Cell culture was incubated and periodically controlled for observing cell adhesion. In terms of rate of cell confluency, medium was changed approximately every three days. When the cells were reached enough (70-80%) confluency; they were detached with 0.25 % (w/v) Trypsin/EDTA (Sigma) solution and harvested, then they were seeded in the larger flask.

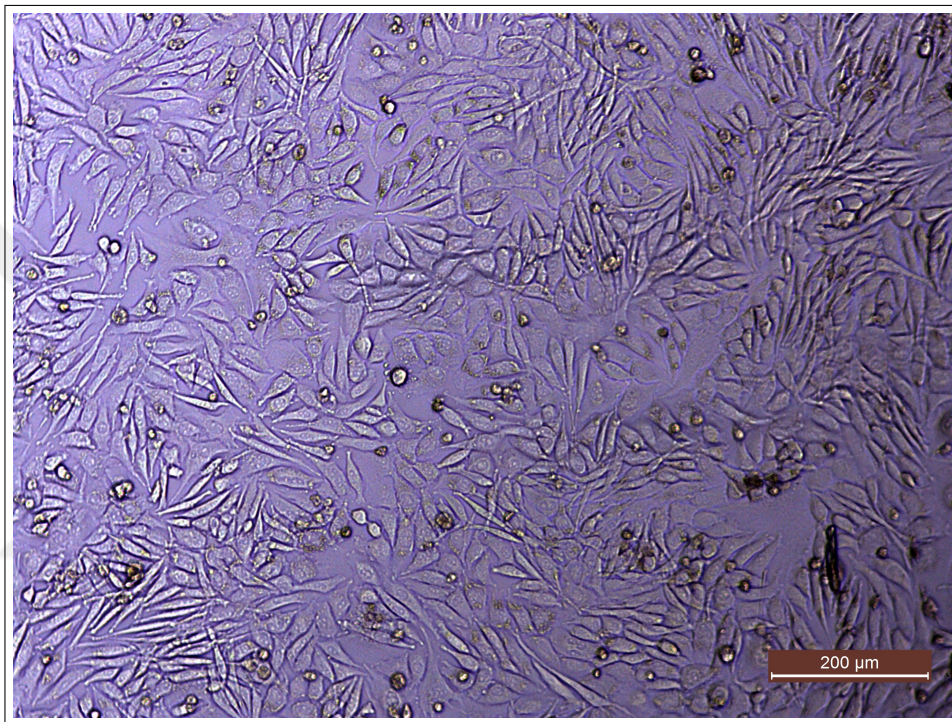


Figure 3.2 Mouse fibroblast (L929) cell line cultured into 96 well-plates.

Before laser irradiation, they were required to be sub-cultured into 96 well-plates for being prepared the analysis procedure. The initial step of the process was that growth medium and Trypsin were warmed up to 37°C inside the water bath. After cell culture flask was placed inside the laminar flow cabin, supernatant fluid was removed from the cell culture flask. A little of phosphate-buffered saline (PBS) solution was added to the flask to cover the bottom area. The flask was swirled; all cells were rinsed with PBS, immediately after PBS was aspirated. Regarding the flask volume, the flask bottom was covered by Trypsin, and it was leaved in incubator to help cell detachment. It was put in incubator and stayed in there about 2 minutes. When the flask was again placed in laminar flow cabin, the medium whose amount was at least

similar to the volume of Trypsin was added on the cells. After pipetting and spraying onto the cell adhered surface of flask, the content was transferred into the centrifuge tube, and spun at 1000 rpm for 5 minutes. The supernatant was removed from the sediment. Appropriate amount of the medium approximately 3-5 ml was added to it. To disperse cell mass into the medium homogenously, the solution was gently pipetting up and down. Before seeding the cell on to the 96 well-plate, cells were required to be counted for meeting the standard confluency.

For cell counting procedure, both rectangular cover slip and Thoma slide (hemocytometer) were placed into the laminar flow cabin, and the rectangular cover slip was put over the Thoma slide. $10\mu\text{l}$ dispersed solution from cell suspension was pipetted between the cover slip and the Thoma slide through the slits on both sides. Before taking each sample to avoid settled, cell suspension was shaken gently. After taking each sample, used pipette tip was changed. The cells were counting within the Thoma grid via optical microscope in both chambers. These were repeated the numbers are consistent.

In the final stage, $100\ \mu\text{l}$ of cell solution was added to the wells. Cells were plated 20,000 cells/well in a 96-well plate. The wells were divided into four groups: non-irradiated (control), $1\ \text{J}/\text{cm}^2$, $3\ \text{J}/\text{cm}^2$, and $5\ \text{J}/\text{cm}^2$. Regarding the conducted investigation, irradiated cells were incubated for 24 h, 48 h, 72 h, separately, after the laser irradiation.

3.2 Laser Irradiation

Laser irradiation was carried out with diode laser at 635 nm (VA-I-400-635, Optotronics-USA). By reading the measurements from optical power meter (1918-R, Newport Corp., CA, USA), the laser system was operated at $50\ \text{mW}/\text{cm}^2$, $125\ \text{mW}/\text{cm}^2$, and $200\ \text{mW}/\text{cm}^2$, respectively. The selected power densities were determined by the results of the former preliminary study. In the preliminary study, the irradiation was occurred at $30\ \text{mW}/\text{cm}^2$, $50\ \text{mW}/\text{cm}^2$, $125\ \text{mW}/\text{cm}^2$, and $200\ \text{mW}/\text{cm}^2$, separately.

According to results of the preliminary study, the minimum threshold of power density was 50 mW/cm^2 . Consequently, 30 mW/cm^2 of power density was omitted from the parameters of experimental groups of the presented study.

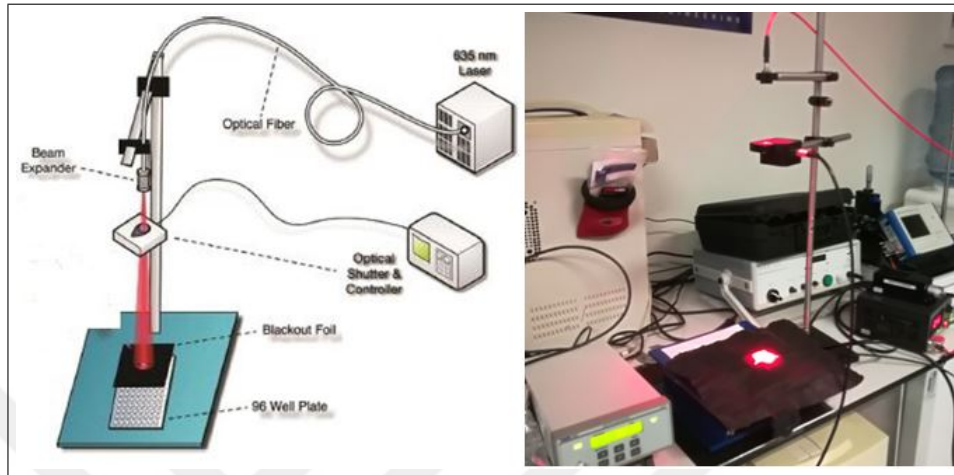


Figure 3.3 LHS scheme represents laser experimental set-up [36], and RHS image shows experimental equipments.

To ensure power density values, each value was repetitively measured by optical power meter, because laser beam and beam expander was moved up and down in order to change the power density for each different laser application. Depending on the value of energy density, cell culturing and irradiation areas in the well plate were organized that represented in Figure 3.4.

The laser setups were positioned above the 96 well plates for homogeneous irradiation at any time. The non-illuminated wells were covered by blackout foil (Thorlabs Inc., NJ, USA). To protect the cells from contamination, the plate was closed by its transparent lid which resulted in power loss; thus, considering, the position of the beam was set accordingly regarding the measurement of power meter by covering the sensorial head of the power meter with a lid of 96-well plate.

Product of each the irradiation time and each power density resulted in different energy density between the laser groups. Experimental groups were positioned on the 96-well plates in terms of the energy density values, shown in Figure 3.4. Sample size of the study was $N=24$.

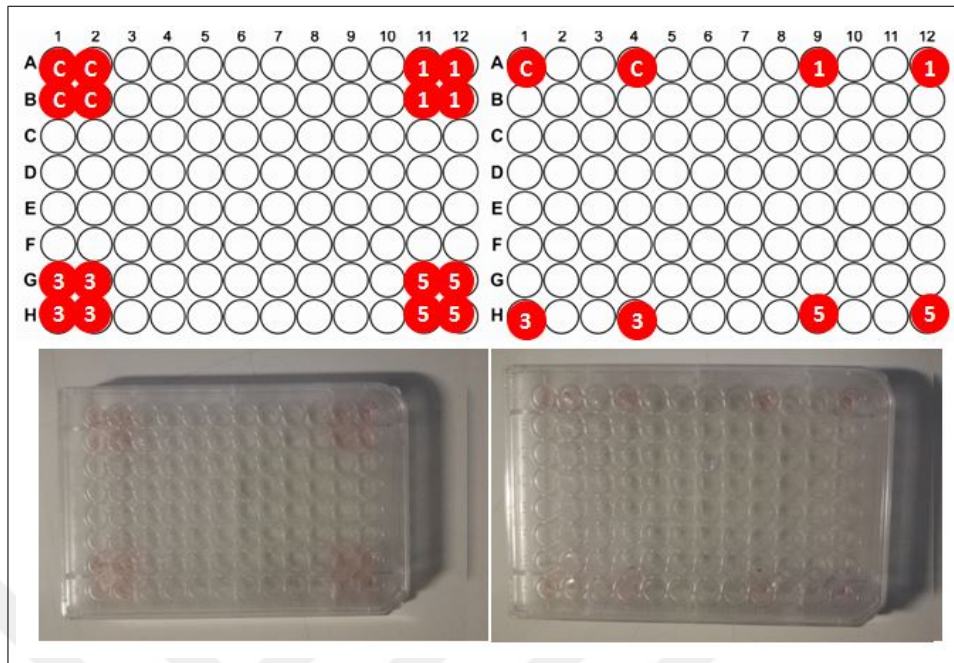


Figure 3.4 Representing the irradiated wells on the plate. The RHS plate displays 125 mW/cm² and 200 mW/cm² laser treatment irradiation; A1 and A4 were control group, the remaining was laser treatment group. On the other hand, The LHS plate was a template of 50 mW/cm² of laser treatment. A1, A2, B1, B2 were the control group, and remaining was laser treatment groups.

Table 3.1
Experimental groups.

Power Density [mW/cm ²]	Energy Density [J/cm ²] = Power Density [mW/cm ²] x Time [sec]			
	0 (control)	1	3	5
50	A0	A1	A3	A5
125	B0	B1	B3	B5
200	C0	C1	C3	C5

Control cells were kept outside of the incubator, and they were under the same condition as the treated cells. Before the laser treatment the medium was changed with PBS solution to eliminate the possibility of interaction between the medium serum and laser light. Each experiment was performed in triplicate.

Table 3.2
Detailed parameters of laser irradiation.

Power Density [mW/cm ²]	Total irradiation time [sec]				Working Distance [cm]	Beam Diameter [cm]
	0 J/cm ²	1 J/cm ²	3 J/cm ²	5 J/cm ²		
50	0 s	20 s	60 s	100 s	40.0	2.5
125	0 s	8 s	24 s	40 s	26.5	1.7
200	0 s	5 s	15 s	25 s	20.7	1.4

3.3 Cell viability (MTT Assay)

Without applying any assay, morphological developments of the cells were observed by inverted microscope (DM IL LED, Leica Microsystems). Cell viability was measured by MTT (3-(4,5-Dimethyliazol-2-yl)-2,5 diphenyltetrazolium bromide) assay at 24 h, 48 h, and 72 h post irradiation. It is a standard quantitative colorimetric method, which measures the reduction of yellow tetrazolium salt to an insoluble purple formazan spectrophotometrically.

MTT stock solution was prepared a 5 mg/ml in PBS, and it was filtered by 20 μ l filter. Incubated growth medium was removed from the plate. 10% v/v of MTT stock solution was added to fresh medium. The volume of MTT can be changed in terms of the number of well. For 96 well plate, 10 μ l solution was added to each filled well. The resultant solution was incubated at 37 °C for 3 hours. The entire medium was removed from the wells. Approximately 100 μ l of dimethyl sulfoxide (DMSO) was added to each well. The plates were covered by aluminum foil, and they were agitated on the shaker for 2-5 min. The optical absorbance which measured by microplate reader (iMark, Bio-Rad) was read at 570 nm, and the reference absorbance was read at 750 nm. To obtain net absorbance values, average absorbance values of blank wells were subtracted from the values of sample wells, and the values were normalized.

3.4 Statistical Analysis

The absorbance values were normalized. By using SPSS (IBM SPSS, Statistics 23 statistical data analysis software), the given distribution were examined by Kolmogorov Simirnov Test to check normal distribution. Experimental results were statistically analyzed by One-way Analysis of Variance (ANOVA) method which was complemented by Tukey's B test and Tamhane's T2 test for statistical comparison. The statistically significance level of difference between the experimental groups were taken as 5% ($p \leq 0.05$).



4. RESULTS AND DISCUSSIONS

4.1 The effect of PBM on L929 cell proliferation with 24 h incubation after laser irradiation

The objective of this stage was to understand the effect of PBM at 635 nm on the mouse fibroblast cell line proliferation with 24h incubation after the laser irradiation via detection assay of cell viability.

Cell viability was analyzed by MTT assay. The resultant values were normalized. In the graphs, x-axis demonstrates the experimental groups, and y-axis shows cell viability in terms of the absorbance values.

4.1.1 Irradiation at 50 mW/cm²

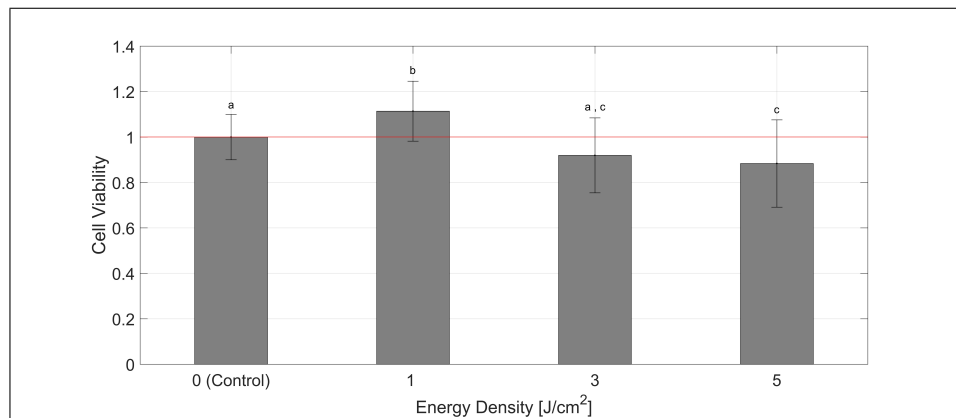


Figure 4.1 Graph shows the results of normalized absorbance values of cell irradiated at 50 mW/cm² with 24 h incubation post irradiation.

There was a statistically significant increase in the irradiation dose of 1 J/cm² compared to the control group. In addition, the most effective intensity value among the irradiated groups is 1 J/cm² and the value that became statistically higher than the other treated groups. Although there was a decrease in between 3 J/cm² and 5 J/cm²

Table 4.1
Quantitative experimental data at 50 mW/cm² irradiation with 24 h incubation.

	Control	1 J/cm²	3 J/cm²	5 J/cm²
Mean	1.00000	1.11367	0.91916	0.88351
Standard Deviation	0.09995	0.13186	0.16491	0.19209

laser irradiated groups, the difference between them was not significant. While 3 J/cm² had inhibitory effect when comparing with control group, 5 J/cm² affects remarkably adversely on cell viability compared to control group.

4.1.2 Irradiation at 125 mW/cm²

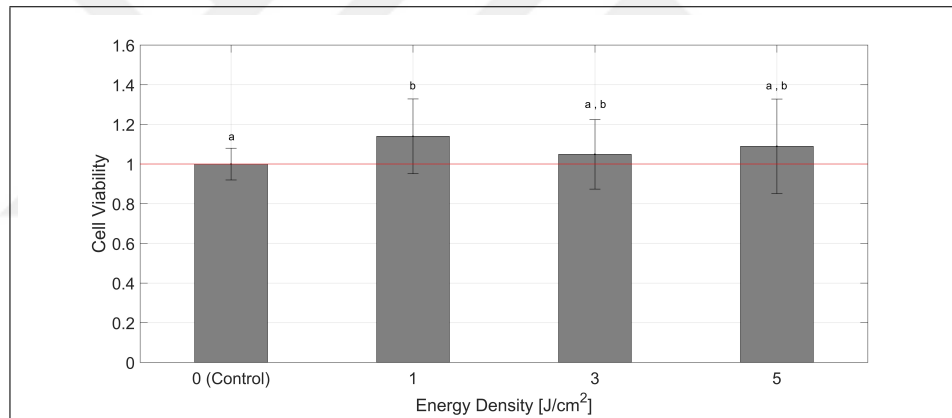


Figure 4.2 Graph shows the results of normalized absorbance values of cell irradiated at 125 mW/cm² with 24 h incubation post irradiation.

Table 4.2
Quantitative experimental data at 125 mW/cm² irradiation with 24 h incubation.

	Control	1 J/cm²	3 J/cm²	5 J/cm²
Mean	1.00000	1.13991	1.04897	1.08935
Standard Deviation	0.08010	0.18829	0.17497	0.23838

The results showed that the only statistical difference was between control group and 1 J/cm², laser treated group. Each laser irradiated group has the upward trend compared to control group. Among irradiated the cell lines did not significantly differ to each other in terms of their cell viability. However, notwithstanding the slight

difference between the laser groups, 3 J/cm² did not give a very good performance compared to other laser groups.

4.1.3 Irradiation at 200 mW/cm²

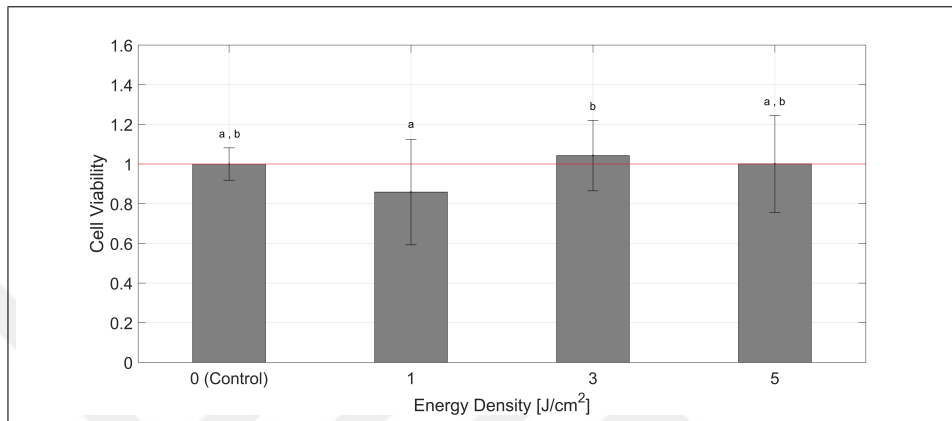


Figure 4.3 Graph shows the results of normalized absorbance values of cell irradiated at 200 mW/cm² with 24 h incubation post irradiation.

Table 4.3

Quantitative experimental data at 200 mW/cm² irradiation with 24 h incubation.

	Control	1 J/cm ²	3 J/cm ²	5 J/cm ²
Mean	1.00000	0.85884	1.04282	1.00102
Standard Deviation	0.08160	0.26623	0.17814	0.24489

The outcomes of the experiment display that there was no significant difference between control group and each laser irradiated groups. Interestingly, for the other applied intensity values, 1 J/cm² was the most proliferative dose among them; however for irradiation at 200 mW/cm², the decrease was noticeable. In spite of the apparent decline of 1 J/cm², the only statistical difference was occurred in between 1 J/cm² and 3 J/cm². In addition, for 50 mW/cm² and 125 mW/cm² irradiation, 5 J/cm² had an inhibitory effect; meanwhile, the viability of cells irradiated at 5 J/cm² with 200 mW/cm² irradiance showed similarity with the control group. Absorbance values of cells treated by laser with energy density at 3 J/cm² and 5 J/cm² were nearly close to each other.

4.2 The effect of PBM on L929 cell proliferation with 48 h incubation after laser irradiation

The aim of this stage was to comprehend the impact of PBM at 635 nm on the mouse fibroblast cell line proliferation with 48 h incubation after the laser illumination by analysis of cell viability test.

Cell viability was examined by MTT test. The resultant qualities were normalized. In the graphs, x-axis exhibits the experimental groups, and y-axis indicates cell viability regarding the absorbance rates.

4.2.1 Irradiation at 50 mW/cm²

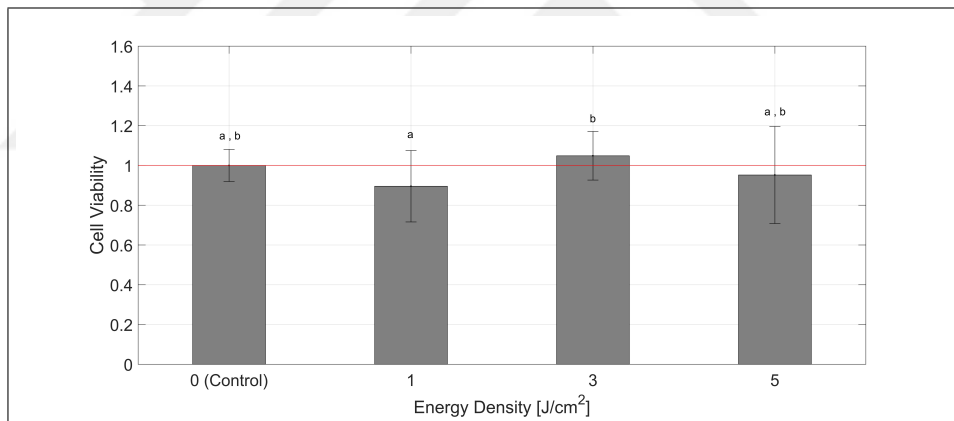


Figure 4.4 Graph shows the results of normalized absorbance values of cell irradiated at 50 mW/cm² with 48 h incubation post irradiation.

Table 4.4

Quantitative experimental data at 50 mW/cm² irradiation with 48 h incubation.

	Control	1 J/cm ²	3 J/cm ²	5 J/cm ²
Mean	1.00000	0.89549	1.04851	0.95187
Standard Deviation	0.08070	0.17960	0.12238	0.24395

The resultant graph reveals that there was statistically significant difference between 1 J/cm² and 3 J/cm² of laser illumination at 50 mW/cm² of power density with 48 h incubation after laser performance on the cells. Avowedly, laser application at 200

mW/cm² with 24 h incubation period after laser illumination and laser application at 50 mW/cm² with 48 h incubation of post laser application might affect the cell viability of the fibroblasts in similar manner. Unlike the mentioned situation, at this intensity value, the dose of 5 J/cm² had a little restraining effect on the cell division. Between the control group and the each laser treated groups, the significant different was not observed. Depending on the absorbance values of the laser fluence at 3 J/cm², proliferation of the fibroblast cells was triggered compared to control group and the other laser groups. Strikingly, according to the results, there was no consistency between the values resulted from laser illumination at 50 mW/cm² of the power density with 24 h incubation time and 48 h incubation time after the laser performance. On account of that for 24 h of incubation interval after laser illumination at 50 mW/cm², the most stimulative dose was 1 J/cm², unlike 48 h of incubation interval.

4.2.2 Irradiation at 125 mW/cm²

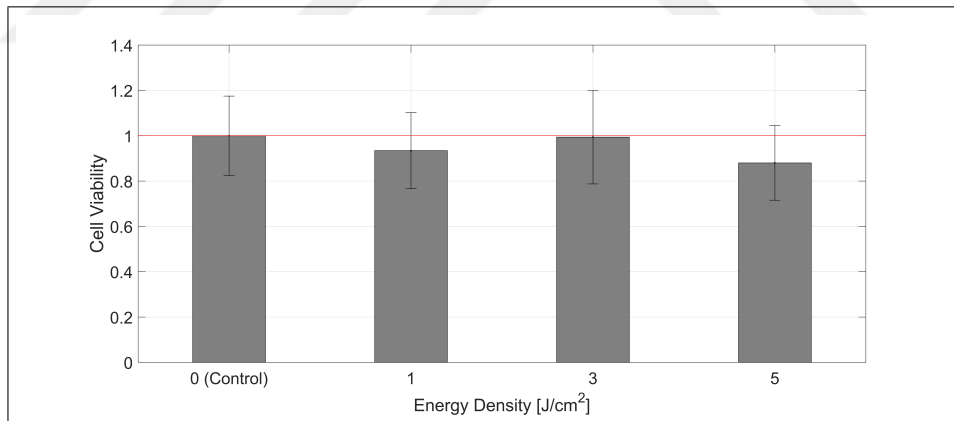


Figure 4.5 Graph shows the results of normalized absorbance values of cell irradiated at 125 mW/cm² with 48 h incubation post irradiation.

Table 4.5

Quantitative experimental data at 125 mW/cm² irradiation with 48 h incubation.

	Control	1 J/cm ²	3 J/cm ²	5 J/cm ²
Mean	1.00000	0.93407	0.99394	0.87990
Standard Deviation	0.08070	0.17960	0.12238	0.24395

Illumination at $125\text{mW}/\text{cm}^2$ with 48 h incubation post laser application did not reveal statistical difference between the groups including control group and laser groups. Laser groups of 48 h incubated cells had less viability compared to laser groups of 24 h incubated cells. Unlike 24 h incubation after laser irradiation, every values belonging to the experimental group were slightly declined in contrast with the control group of 48 h incubation after laser applications. The nearest value among the laser groups to the control group was irradiated cell group by $3\text{ J}/\text{cm}^2$ of energy density. On the other hand, treated cells with $5\text{ J}/\text{cm}^2$ diminished in viability. Like the effect of the fluence of $5\text{ J}/\text{cm}^2$ on cell viability, the dose of $1\text{ J}/\text{cm}^2$ had similar effect on the irradiated cells.

4.2.3 Irradiation at $200\text{ mW}/\text{cm}^2$

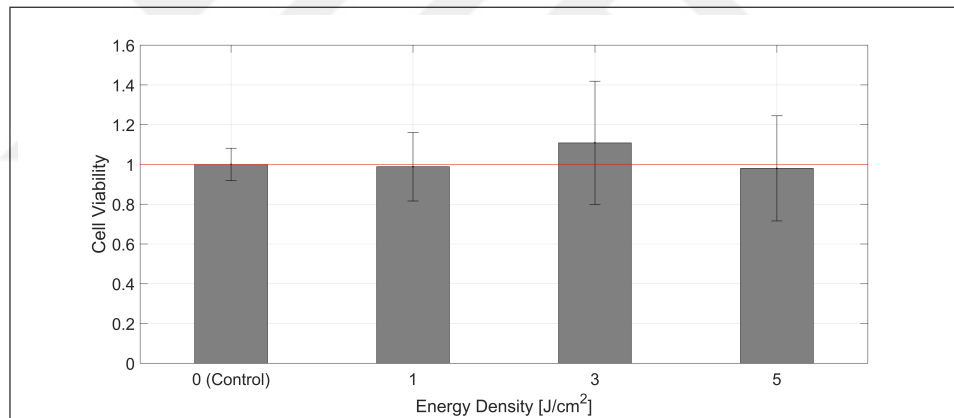


Figure 4.6 Graph shows the results of normalized absorbance values of cell irradiated at $200\text{ mW}/\text{cm}^2$ with 48 h incubation post irradiation.

Table 4.6
Quantitative experimental data at $200\text{ mW}/\text{cm}^2$ irradiation with 48 h incubation.

	Control	$1\text{ J}/\text{cm}^2$	$3\text{ J}/\text{cm}^2$	$5\text{ J}/\text{cm}^2$
Mean	1.00000	0.98835	1.10836	0.98880
Standard Deviation	0.08186	0.17248	0.31055	0.26450

For this intensity value, no statistical difference was occurred in between the experimental groups. At first glance, population of cells irradiated at $3\text{ J}/\text{cm}^2$ was increased by laser application in comparison with control group and the other laser

groups. Except for the group representing the irradiation at 3 J/cm^2 , both non-irradiated group and the laser groups' results were very close to each other. In terms of the comparison between the incubation intervals of 24 h and 48 h, there was a difference between the levels of the bar charts since the shortest incubation interval caused notable inhibition on the cell viability. However, 48 h incubation interval with 1 J/cm^2 irradiation did not performed apparent inhibitory effects on the cell viability.

4.3 The effect of PBM on L929 cell proliferation with 72 h incubation after laser irradiation

The point of this examination was to grasp the effect of PBM at 635 nm on the mouse fibroblast cell line proliferation with 72 h incubation after the laser light by the methods for cell viability test.

Cell viability was inspected by MTT test. The resultant characteristics were normalized. In the bar charts, horizontal axis displays the experimental groups, and vertical axis shows cell viability with regards to the absorbance values.

4.3.1 Irradiation at 50 mW/cm^2

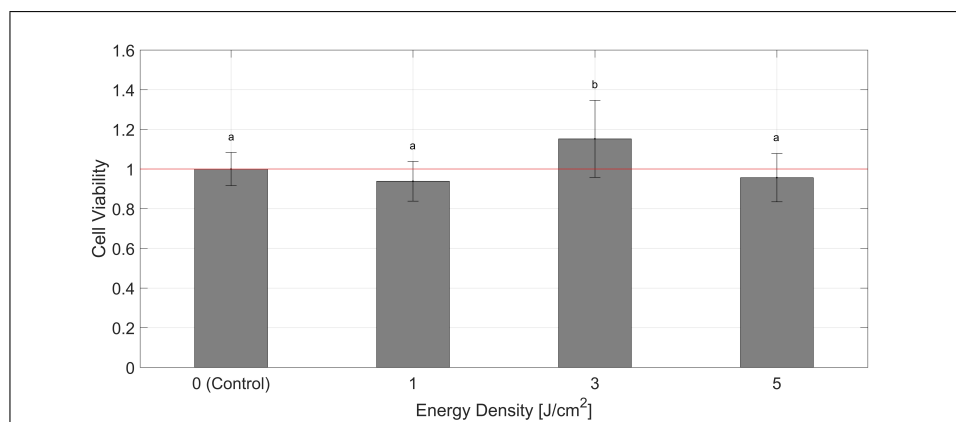


Figure 4.7 Graph shows the results of normalized absorbance values of cell irradiated at 50 mW/cm^2 with 72 h incubation post irradiation.

Table 4.7
Quantitative experimental data at 50 mW/cm² irradiation with 72 h incubation.

	Control	1 J/cm ²	3 J/cm ²	5 J/cm ²
Mean	1.00000	0.93832	1.15224	0.95650
Standard Deviation	0.08366	0.10028	0.19433	0.12156

In the graph, Figure 4.7, viability of cells at 3 J/cm² showed the statistical significant difference compared to non-irradiated group and the other laser groups. The dose of 3 J/cm² had the most efficient impact on the cell viability in the experimental groups. Apart from the group representing 3 J/cm² irradiation dose, control group, 1 J/cm² and 5 J/cm², these three groups had similar absorbance rates. However, when the control group was taken as a reference for cell viability, both the groups treated at 1 J/cm² and 5 J/cm² affected adversely on cell viability. If the bar graphs of different incubation intervals of the same intensity value were almost overlapped, it was obvious that 24 h incubation differs from the others; on the other hand, other two resembled to each other.

4.3.2 Irradiation at 125 mW/cm²

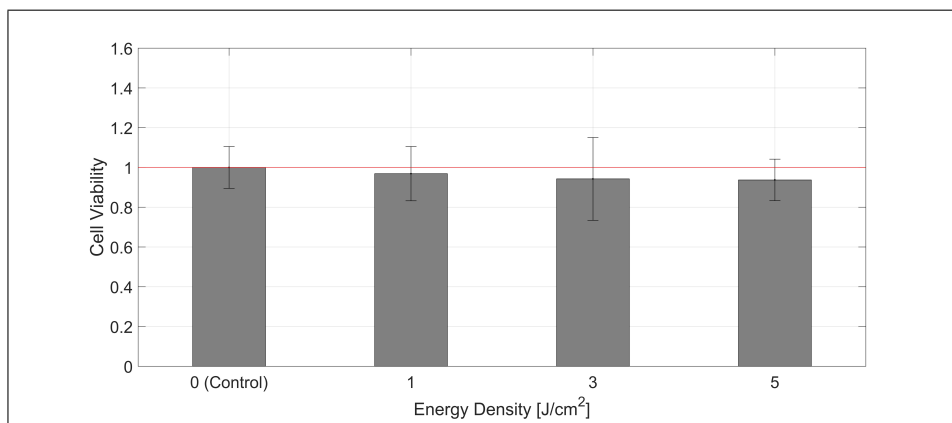


Figure 4.8 Graph shows the results of normalized absorbance values of cell irradiated at 125 mW/cm² with 72 h incubation post irradiation.

There was no statistically significant difference between the experimental groups. The bar chart represents the slight decrease in the cell viability. In terms of the analysis

Table 4.8
Quantitative experimental data at 125 mW/cm² irradiation with 72 h incubation.

	Control	1 J/cm²	3 J/cm²	5 J/cm²
Mean	1.00000	0.96851	0.94227	0.93714
Standard Deviation	0.10506	0.13637	0.20819	0.10433

of the assay, as the laser radiation dose was increased, correspondingly, cell viability slightly decreased.

4.3.3 Irradiation at 200 mW/cm²

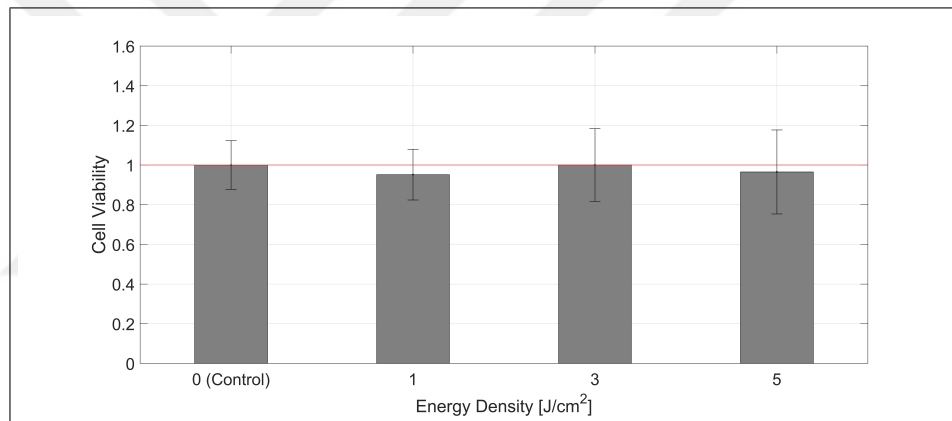


Figure 4.9 Graph shows the results of normalized absorbance values of cell irradiated at 200 mW/cm² with 72 h incubation post irradiation.

Table 4.9
Quantitative experimental data at 200 mW/cm² irradiation with 72 h incubation.

	Control	1 J/cm²	3 J/cm²	5 J/cm²
Mean	1.00000	0.95149	1.00053	0.96522
Standard Deviation	0.12242	0.12785	0.18312	0.21184

In spite of little fluctuation between the groups, there was no statistical significant difference between the experimental groups. Absorbance of each treated experimental group was very close to non-illuminated group. Depending on the mean values, 1 J/cm² resulted in more restrictor effect on cell viability, and energy density of 3 J/cm² irradiation caused more proliferative effect compared to the other groups. In

terms of comparing the different incubation intervals post irradiation at 200 mW/cm², both the three graphs were shown in similar shift between the groups; however, the rates of absorbance change were varied.

4.4 Results Overview

The summary of experimental results was displayed in the Table 4.10. The stated summarized results showing the statistically significant differences, as far as it was applicable. In order to determine the significance between the groups, the measurements of absorbance of laser groups were compared to their own control groups.

Table 4.10

The outcomes of the presented study in a nutshell. "P", "I", and "N" denote proliferative, inhibitory, and no effect on cell viability, respectively.

	L929 cells in vitro, Laser irradiation at 635 nm, Results of MTT assay								
	24h			48h			72h		
	1 J/cm ²	3 J/cm ²	5 J/cm ²	1 J/cm ²	3 J/cm ²	5 J/cm ²	1 J/cm ²	3 J/cm ²	5 J/cm ²
50 mW/cm ²	P	N	I	N	N	N	N	P	N
125 mW/cm ²	P	N	N	N	N	N	N	N	N
200 mW/cm ²	N	N	N	N	N	N	N	N	N

As it is seen in Table 4.10, the effect of PBM was altered by power density, energy density and incubation time after laser irradiation. Although the study conducted was aimed to find out the minimum and maximum limits of effective power densities, only 50 mW/cm² of power density might be inducted as a minimum threshold value. On the other hand, 125 mW/cm² and 200 mW/cm² of power densities were unpredictable values to introduce as a maximum limit of efficacy of PBM since the results did not give enough information to put an interpretation on the issue.

The outcomes clearly showed that energy density was not an only parameter that influenced on activation of cell metabolism. Efficiency of energy density was not

independent of power density and incubation interval post illumination. With respect to the results, the remarkable cellular responses were encountered in 24 h and 72 h incubation after laser application.

4.5 Discussion

The variation efficacy of power densities had an important impact on the results of this research. Although the laser fluences were kept constant for all experimental groups, the measurements did not show the same effectiveness on the graphs. There might be many causes of these results. Results displayed that even if laser fluence and its intensity values were the same for some groups, incubation interval period post irradiation altered the consequences.

According to, Bunsen - Roscoe Reciprocity Law based on photo-biological response is unrelated to power density and irradiation duration when the product of these elements (i.e. energy density) is constant. Reciprocity law, developed by German chemist/physicist Robert Wilhelm Bunsen and English chemist Sir Henry Enfield Roscoe, is one of the necessary rules of photochemistry. It is claimed that the resultant elements of photochemical reaction is controlled by the laser energy. Predictably, cellular response is independent from the intensity and the exposure time. In accordance with the statement of the study of Karu (1994), this law might not be always valid for some cases. It has been explained that the laser irradiance and exposure time was more significant than the energy density. If a study identifies long terms photobiological research such as proliferation of microorganism, Bunsen - Roscoe Law might be invalid. Concerning that when signals of absorbed laser light are converted in photobiological responses, growth stimulation is occurred, which is controlled by two distinct parameters which are irradiation dose (power density) and irradiation time [52]. Likewise, the presented Table 4.10 presents that even though the product of power density and exposure time keep constant, the cellular response can change. For instance, although 50 mW/cm^2 and 125 mW/cm^2 had the same efficiency on proliferation at 1 J/cm^2 irradiation in the same incubation period, their resulting effects at 5 J/cm^2 ir-

radiation differed from each other. In addition, the difference between the effects of intensity values on cellular response was also observed with the other energy densities and incubation times.

It is hard to compare the outcomes of this study with the remarks of other researches in the literature; since the most of them have been acknowledging energy density of laser light as the optimal parameter, whereas the presented study examined the relation between power density and energy density. According to the results, different power densities create different impact on efficiency of energy densities, and the incubation time is also a dependent variable for efficacy of PBM. Therefore, my study can only be compare with previous studies regarding energy density and power density, separately, since the treatment combination of power density, energy density and incubation time post irradiation are not mentioned in previous studies.

According to Arndt-Schulz Curve, the most beneficial impact on cell activation starts with EMR at 1 J/cm^2 , and maintains the effects until reaching 4 J/cm^2 . After exceeding this limit, the stimulative impact is retarded slowly [35]. However, the results of the presented study was not completely correlated with the curve, since despite the therapeutic window which is apparently defined as $3\text{-}4 \text{ J/cm}^2$, 1 J/cm^2 irradiation at 50 mW/cm^2 causes significant increase in cell proliferation. In fact, the curve shows that 1 J/cm^2 irradiation results in steady-state response in cell activation, but the proliferative effect of 1 J/cm^2 changed with different incubation time post irradiation in terms of the results.

Incubation time post laser irradiation should be considered since it is one of important factors to define the performance of the irradiation. Solmaz et al. (2017) reported that for the L929 cell viability of 24 h incubated cells, 635 nm laser light at 1 J/cm^2 and 3 J/cm^2 energy density with 50 mW output power significantly increased in cell proliferation compared to the control group. Likewise, the presented results in Table 4.10 shows that 1 J/cm^2 of irradiation at 50 mW/cm^2 increased cell viability, but 3 J/cm^2 did not cause any significant effect. In his study, 1 J/cm^2 irradiation in 72 h incubation period post laser illumination significantly raised the proliferative impact of

cellular metabolic activation comparing with the non-irradiated group. Whereas, the results, shown in Table 4.10, indicate that only the laser treatment at 3 J/cm^2 with 50 mW/cm^2 power density had positive effect on cell viability. In addition, there was also no statistical significant difference between the experimental groups which incubated for 48 h after the laser application for both these two studies [36].

Some authors recommended longer incubation time after the laser applications. However, stimulative effects of laser light might be declined in time because of reaching the maximum limit of the proliferation of the cells in a culture medium [53]. Regarding this, some authors proposed that 1-3 hours of incubation time is enough to take measurements, to observe and analyze them [54]. Moreover, the efficacy of incubation interval on cell proliferation can be based on a cellular behavior. According to Simpson et al. (2013), after 24 h of observation showed that murine fibroblast cells (i.e. 3T3 cell line) had a tendency to be motile; on the contrary, after 72 h of observation, a number of cells were increased by cell proliferation. In the mentioned study, the researchers used in vitro wound model and mathematical modeling experiments with barrier assay [15]. As stated by the results of presented study in Table 4.10, there was no difference between the control cell group and treated cell groups that incubated for 72 h, except for cells irradiated at 3 J/cm^2 . Correspondingly, this "none effect" might be the result of mentioned cellular behavior. In other words, in progress of time, non-irradiated cells might also tend to proliferate rapidly.

Alternatively, it is also possible to apply laser treatment for three following days without any examination. In this case, observation can be done at the end of three days, instead of incubating cells for three consecutive days with the examination done at the end of each day. According to study of Basso et al., human gingival fibroblast cells were treated with $780 \text{ nm} \pm 3 \text{ nm}$ and 0.04 W maximum output power of laser light at the fluences of $0.5, 1.5, 3, 5, 7 \text{ J/cm}^2$. The laser light performed at 24 h, 48 h, and 72 h without daily examination. As a result, in comparison with the control group, 0.5 J/cm^2 and 3 J/cm^2 led to rise in cell viability significantly as opposed to 1.5 J/cm^2 and 7 J/cm^2 which inhibited the cell activity. Likewise, as reported by the presented study, 3 J/cm^2 irradiation induced cell proliferation with applying the

nearest power values that used in Basso's research, but this proliferative effect was observed in only 72 h incubation post illumination. However, non-irradiated group did not necessarily differ from the laser treated group at 5 J/cm² [42]. Alike, Table 4.10 indicates that cells treated with 5 J/cm² of energy density and 50 mW/cm² of power density were affected neither positively nor negatively except for cells incubated in 24 h period post irradiation.

The efficacy of PBM depends on using standardized parameters, and the most efficient values of laser light vary in between 1 - 1000 mW [34]. Illescas-Montes et al. conducted a study; laser illumination was applied to human epithelial fibroblast cells (CCD-1064SK). Applied power values were 0.2 W, 0.5 W, and 1 W; energy densities were varied in between 1-7 J/cm². In addition, irradiated cells were incubated for 24 h or 72 h, separately. It was stated that a power of 0.2 W or 0.5 W, and energy densities within 1 J/cm² to 4 J/cm² (i.e. including 1, 2, 3, 4 J/cm²) were the most proliferative parameters for both 24 h and 72 h incubation interval [55]. Similarly, in the presented study, cellular metabolic activation increased at 50 mW/cm² and 125 mW/cm² of power densities for 1 J/cm² of energy density with 24 h incubation. It was also raised by irradiation at 3 J/cm² and 50 mW/cm² of power density with 72 h incubation.

In addition to effects of optimal parameters on the cellular response, the extra stress conditions, endogenous or exogenous, enable system to support its own healing mechanism. Ayuk et al. addressed that laser irradiation (660 nm) at 5 J/cm² with the power density of 11.23 mW/cm² was not harmful on stressed cells (WS1, human skin fibroblasts) such as normal wounded, diabetic wounded, hypoxic wounded and diabetic hypoxic wounded. The study groups clarified that PBM supports to enhancing cell metabolism and increasing proliferation for healing in 48 h incubation post irradiation [56]. However, Table 4.10 shows that 5 J/cm² of energy density did not have any effect on cellular metabolic activation in 48 h incubation for all power density values.

As stated in the background section, the mechanism of PBM is related to mitochondrial reactions. In addition to photochemical reactions, there are a few factors

that affect metabolism of a cell and the cellular response. Therefore, many different factors should always be considered before conducting a study.



5. CONCLUSION

The aim of the study was to grasp the effect of different power densities of laser light (at 635 nm) on cell proliferation in vitro by changing exposure time of laser. Another focusing point was to understand the impact of incubation time post irradiation affected on cell division.

The addressed study was a multi-comparative study. There were comparisons between selected energy, power densities, and incubation interval after laser application, separately. According to the results stated, cellular response to laser irradiation can be changed by intensity of laser light. In addition, although the energy density and the power density of laser light that applied to the cells was constant, the parameters activated the metabolism of cells in the long term, which can be concluded that incubation time has an importance on efficacy of PBM.

The contradictory outcomes might be resulted from determined parameters used in the experiments. PBM is a biphasic photochemical application. Thus, it is highly dose dependent. Like Arndt- Schulz Curve, it is required that the other parameters of laser irradiation should be established as a formulation or a graphical representation in order to clarify the effects of the parameters.

For years, PBM have been using as a therapeutic application to trigger cell division. Besides the benefits of this treatment, lack of standard laboratory equipment and the efficiently reported data can create suspicious that PBM is completely safe. Clearly, the actual effect of this application cannot be understood by looking at some limited parameters. As seen in the conducted in vitro study, results can alter, when only a factor is changed. When this application is used in in vivo model, the experiments should be designed with this consideration. If these studies are followed by clinical trials, the selection of parameters and the definition of treatment duration should be decided wisely.

For future studies, same standard procedures should be introduced into in vivo model.



REFERENCES

1. Goldman, L., *The History and Development of the Medical Laser*, pp. 3–7. Boston, MA: Springer US, 1990.
2. Swedish Laser Medical Society, “FAQ - Frequently Asked Questions About Laser Therapy.”
3. Laakso, L., C. Richardson, and T. Cramond, “Factors affecting Low Level Laser Therapy,” *Australian Journal of Physiotherapy*, Vol. 39, no. 2, pp. 95–99, 1993.
4. Jenkins, P. A., and J. D. Carroll, “How to Report Low-Level Laser Therapy (LLLT)/Photomedicine Dose and Beam Parameters in Clinical and Laboratory Studies,” *Photomedicine and Laser Surgery*, Vol. 29, pp. 785–787, dec 2011.
5. Chow, R. T., “Dose Dilemmas in Low Level Laser Therapy - The Effects of Different Paradigms and Historical Perspectives,” *Laser Therapy*, Vol. 13, no. 1, pp. 102–109, 2000.
6. Nilforoushzadeh, M. A., H. R. Ahmadi Ashtiani, F. Jaffary, F. Jahangiri, N. Nikkhah, M. Mahmoudbeyk, M. Fard, Z. Ansari, and S. Zare, “Dermal Fibroblast Cells: Biology and Function in Skin Regeneration,” *Journal of Skin and Stem Cell*, Vol. In Press, jun 2017.
7. Tracy, L. E., R. A. Minasian, and E. Caterson, “Extracellular matrix and dermal fibroblast function in the healing wound,” *Advances in Wound Care*, Vol. 5, no. 3, pp. 119–136, 2016.
8. Omelchenko, T., J. M. Vasiliev, I. M. Gelfand, H. H. Feder, and E. M. Bonder, “Mechanisms of polarization of the shape of fibroblasts and epitheliocytes: Separation of the roles of microtubules and Rho-dependent actin-myosin contractility,” *Proceedings of the National Academy of Sciences*, Vol. 99, pp. 10452–10457, aug 2002.
9. Abercrombie, M., “Fibroblasts,” *Journal of Clinical Pathology*, Vol. s3-12, pp. 1–6, jan 1978.
10. Hyland, K., “Cell Proliferation and Its Regulation (Biochemistry/Molecular Biology Lecture),” 2018.
11. Australian Government, *Normal Cell Proliferation*, 2014.
12. Australian Government, *Abnormal Cell Proliferation*, 2014.
13. Cooper, G. M., *The Cell: A Molecular Approach. 2nd edition*, 2000.
14. Otterço, A., A. Andrade, P. Brassolatti, K. Pinto, H. Araújo, and N. Parizotto, “Photobiomodulation mechanisms in the kinetics of the wound healing process in rats,” *Journal of Photochemistry and Photobiology B: Biology*, Vol. 183, pp. 22–29, jun 2018.
15. Simpson, M. J., K. K. Treloar, B. J. Binder, P. Haridas, K. J. Manton, D. I. Leavesley, D. L. S. McElwain, and R. E. Baker, “Quantifying the roles of cell motility and cell proliferation in a circular barrier assay,” *Journal of The Royal Society Interface*, Vol. 10, pp. 20130007–20130007, feb 2013.

16. Fodor, L., Y. Ullmann, and M. Elman, "Light Tissue Interactions," in *Aesthetic Applications of Intense Pulsed Light*, pp. 11–20, London: Springer London, 2011.
17. Prasad, P. N., "Fundamentals of Light-Matter Interactions," in *Introduction to Biophotonics*, 2004.
18. Tuchin, V. V., "Tissue Optics and Photonics: Light-Tissue Interaction," *Journal of Biomedical Photonics & Engineering*, pp. 98–134, jun 2015.
19. Tuchin, V., "Tissue Optics and Photonics: Light-Tissue Interaction II," *Journal of Biomedical Photonics & Engineering*, Vol. 2, no. 3, p. 030201, 2016.
20. Juzeniene, A., P. Brekke, A. Dahlback, S. Andersson-Engels, J. Reichrath, K. Moan, M. F. Holick, W. B. Grant, and J. Moan, "Solar radiation and human health," *Reports on Progress in Physics*, Vol. 74, p. 066701, jun 2011.
21. Farkas, J. P., J. E. Hoopman, and J. M. Kenkel, "Five Parameters You Must Understand to Master Control of Your Laser/Light-Based Devices," *Aesthetic Surgery Journal*, Vol. 33, pp. 1059–1064, sep 2013.
22. Ash, C., M. Dubec, K. Donne, and T. Bashford, "Effect of wavelength and beam width on penetration in light-tissue interaction using computational methods," *Lasers in Medical Science*, Vol. 32, pp. 1909–1918, nov 2017.
23. Vilaseca, M., "Laser Therapy," *Be-Optical*, 2017.
24. Il'ichev, Y. V., "Photochemistry: Theoretical Concepts and Reaction Mechanisms," 2008.
25. Chan, B. P., "Biomedical Applications of Photochemistry," *Tissue Engineering Part B: Reviews*, Vol. 16, pp. 509–522, oct 2010.
26. Steiner, R., "Laser-Tissue Interactions," in *Laser and IPL Technology in Dermatology and Aesthetic Medicine*, pp. 23–36, Berlin, Heidelberg: Springer Berlin Heidelberg, 2011.
27. Hamblin, M. R., "Mechanisms and applications of the anti-inflammatory effects of photobiomodulation," *AIMS Biophysics*, Vol. 4, no. 3, pp. 337–361, 2017.
28. Passarella, S., and T. Karu, "Absorption of monochromatic and narrow band radiation in the visible and near IR by both mitochondrial and non-mitochondrial photoacceptors results in photobiomodulation," *Journal of Photochemistry and Photobiology B: Biology*, Vol. 140, pp. 344–358, nov 2014.
29. Houeild, N. N., R. T. Masha, and H. Abrahamse, "Low-intensity laser irradiation at 660 nm stimulates cytochrome c oxidase in stressed fibroblast cells," *Lasers in Surgery and Medicine*, Vol. 44, pp. 429–434, jul 2012.
30. Karu, T. I., "Cellular and Molecular Mechanisms of Photobiomodulation (Low-Power Laser Therapy)," *IEEE Journal of Selected Topics in Quantum Electronics*, Vol. 20, pp. 143–148, mar 2014.
31. Karoussis, I. K., K. Kyriakidou, C. Psarros, M. Koutsilieris, and J. A. Vrotsos, "Effects and Action Mechanism of Low Level Laser Therapy (LLLT): Applications in Periodontology," *Dentistry*, Vol. 08, no. 09, 2018.

32. Karu, T. I., "Mitochondrial Signaling in Mammalian Cells Activated by Red and Near-IR Radiation," *Photochemistry and Photobiology*, Vol. 84, pp. 1091–1099, sep 2008.
33. Karu, T., "Primary and secondary mechanisms of action of visible to near-IR radiation on cells," *Journal of Photochemistry and Photobiology B: Biology*, Vol. 49, pp. 1–17, mar 1999.
34. Chung, H., T. Dai, S. K. Sharma, Y.-Y. Huang, J. D. Carroll, and M. R. Hamblin, "The Nuts and Bolts of Low-level Laser (Light) Therapy," *Annals of Biomedical Engineering*, Vol. 40, pp. 516–533, feb 2012.
35. Sommer, A. P., A. L. B. Pinheiro, A. R. Mester, R.-P. Franke, and H. T. Whelan, "Bios-timulatory Windows in Low-Intensity Laser Activation: Lasers, Scanners, and NASA's Light-Emitting Diode Array System," *Journal of Clinical Laser Medicine & Surgery*, Vol. 19, pp. 29–33, feb 2001.
36. Solmaz, H., Y. Ulgen, and M. Gulsoy, "Photobiomodulation of wound healing via visible and infrared laser irradiation," *Lasers in Medical Science*, Vol. 32, pp. 903–910, may 2017.
37. Sardari, F., and F. Ahrari, "The effect of low-level helium-neon laser on oral wound healing," *Dental Research Journal*, Vol. 13, no. 1, p. 24, 2016.
38. Lau, P., N. Bidin, G. Krishnan, S. M. AnaybBaleg, M. B. M. Sum, H. Bakhtiar, Z. Nassir, and A. Hamid, "Photobiostimulation effect on diabetic wound at different power density of near infrared laser," *Journal of Photochemistry and Photobiology B: Biology*, Vol. 151, pp. 201–207, oct 2015.
39. Marques, J. M., C. Pacheco-Soares, and N. S. D. Silva, "Evaluation of the photobiomodulation in L929 cell culture," *Experimental Biology and Medicine*, Vol. 239, pp. 1638–1643, dec 2014.
40. Kilík, R., L. Lakyová, J. Sabo, P. Kruzliak, K. Lacjaková, T. Vasilenko, M. Vidová, F. Longauer, and J. Radonak, "Effect of Equal Daily Doses Achieved by Different Power Densities of Low-Level Laser Therapy at 635 nm on Open Skin Wound Healing in Normal and Diabetic Rats," *BioMed Research International*, Vol. 2014, pp. 1–9, 2014.
41. Esmaelinejad, M., M. Bayat, H. Darbandi, M. Bayat, and N. Mosaffa, "The effects of low-level laser irradiation on cellular viability and proliferation of human skin fibroblasts cultured in high glucose mediums," *Lasers in Medical Science*, Vol. 29, pp. 121–129, jan 2014.
42. Basso, F. G., T. N. Pansani, A. P. S. Turrioni, V. S. Bagnato, J. Hebling, and C. A. de Souza Costa, "In Vitro Wound Healing Improvement by Low-Level Laser Therapy Application in Cultured Gingival Fibroblasts," *International Journal of Dentistry*, Vol. 2012, pp. 1–6, 2012.
43. Lacjaková, K., N. Bobrov, M. Poláková, M. Slezák, M. Vidová, T. Vasilenko, M. Novotný, F. Longauer, Ä. Lenhardt, J. Bober, M. Levkut, F. Sabol, and P. Gál, "Effects of equal daily doses delivered by different power densities of low-level laser therapy at 670 nm on open skin wound healing in normal and corticosteroid-treated rats: a brief report," *Lasers in Medical Science*, Vol. 25, pp. 761–766, sep 2010.
44. Andrade, F. d. S. d. S. D., R. M. d. O. Clark, and M. L. Ferreira, "Effects of low-level laser therapy on wound healing," *Revista do Colégio Brasileiro de Cirurgiões*, Vol. 41, pp. 129–133, apr 2014.

45. Gál, P., M. Mokrý, B. Vidinský, R. Kilík, F. Depta, M. Harakalová, F. Longauer, Š. Možeš, and J. Sabo, "Effect of equal daily doses achieved by different power densities of low-level laser therapy at 635 nm on open skin wound healing in normal and corticosteroid-treated rats," *Lasers in Medical Science*, Vol. 24, pp. 539–547, jul 2009.
46. Demidova-Rice, T. N., E. V. Salomatina, A. N. Yaroslavsky, I. M. Herman, and M. R. Hamblin, "Low-level light stimulates excisional wound healing in mice," *Lasers in Surgery and Medicine*, Vol. 39, pp. 706–715, oct 2007.
47. Hawkins, D., and H. Abrahamse, "Effect of Multiple Exposures of Low-Level Laser Therapy on the Cellular Responses of Wounded Human Skin Fibroblasts," *Photomedicine and Laser Surgery*, Vol. 24, pp. 705–714, dec 2006.
48. Kreisler, M., A. B. Christoffers, B. Willershausen, and B. D'Hoedt, "Effect of low-level GaAlAs laser irradiation on the proliferation rate of human periodontal ligament fibroblasts: an in vitro study," *Journal of Clinical Periodontology*, Vol. 30, pp. 353–358, apr 2003.
49. Pereira, A. N., C. d. P. Eduardo, E. Matson, and M. M. Marques, "Effect of low-power laser irradiation on cell growth and procollagen synthesis of cultured fibroblasts," *Lasers in Surgery and Medicine*, Vol. 31, pp. 263–267, oct 2002.
50. Enwemeka, C. S., "Attenuation and Penetration of Visible 632.8nm and Invisible Infrared 904nm Light in Soft Tissues," *Laser Therapy*, Vol. 13, no. 1, pp. 95–101, 2000.
51. Kara, C., H. Selamet, C. Gökmenoglu, and N. Kara, "Low level laser therapy induces increased viability and proliferation in isolated cancer cells," *Cell Proliferation*, Vol. 51, p. e12417, apr 2018.
52. Karu, T., O. Tiphlova, R. Esenaliev, and V. Letokhov, "Two different mechanisms of low-intensity laser photobiological effects on Escherichia coli," *Journal of Photochemistry and Photobiology B: Biology*, Vol. 24, pp. 155–161, aug 1994.
53. Khoo, N. K., M. A. Shokrgozar, I. R. Kashani, A. Amanzadeh, E. Mostafavi, H. Sanati, L. Habibi, S. Talebi, M. Abouzaripour, and S. M. Akrami, "In vitro therapeutic effects of low level laser at mRNA level on the release of skin growth factors from fibroblasts in diabetic mice," *Avicenna Journal of Medical Biotechnology*, Vol. 6, no. 2, pp. 113–118, 2014.
54. Hawkins, D., and H. Abrahamse, "How Long After Laser Irradiation Should Cellular Responses be Measured to Determine the Laser Effect?," *Journal of Laser Applications*, Vol. 19, pp. 74–83, may 2007.
55. Illescas-Montes, R., L. Melguizo-Rodríguez, F. Manzano-Moreno, O. García-Martínez, C. Ruiz, and J. Ramos-Torrecillas, "Cultured Human Fibroblast Biostimulation Using a 940 nm Diode Laser," *Materials*, Vol. 10, p. 793, jul 2017.
56. Ayuk, S. M., N. N. Houreld, and H. Abrahamse, "Effect of 660 nm visible red light on cell proliferation and viability in diabetic models in vitro under stressed conditions," *Lasers in Medical Science*, Vol. 33, pp. 1085–1093, jul 2018.